

## APPENDIX I

### SILICON DIODE CRYOGENIC SENSORS

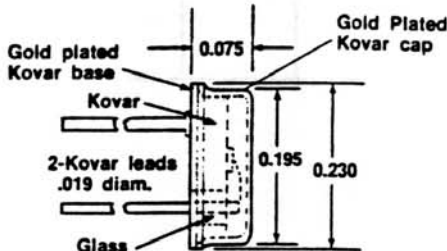
#### Diode Temperature Sensors:

1. Forward voltage measurements should be made at a constant current of 10 or 100 microamperes. The silicon diode can withstand 200 Volts in the reverse direction and up to five milliamperes in the forward direction. In the case of the gallium arsenide diode do not apply a current of greater than one millampere in the forward direction or a voltage of greater than five volts in the reverse direction. Either condition can result in permanent damage to the temperature sensor.

This dangerous condition can be generated specifically with the use of a multimeter type ohmmeter. The solution is straightforward however: For the Simpson 260 types, use the Rx100 ohm scale with a 2 K resistor in series with one lead; for Triplett 630 types, do the same with either the Rx100 or Rx1000 ohm scales. This will limit the back voltage to 1.5 volts and the forward current to less than 1 mA. - yet the forward-reverse difference can easily be seen.

2. If power input to your cryogenic system is critical, the 10 uA current should be used. The power dissipated at helium temperatures by the sensor is approximately 15 microwatts for gallium arsenide and 21 microwatts for silicon for this current. If power input is not critical, then the 100 uA current may be preferred.

3. The static impedance of the silicon diode is 210 K ohms at helium temperatures with 10 microamperes excitation current and 21 K ohms with 100 microampere excitation current. The static impedance of the gallium arsenide sensor at helium temperatures is approximately 150 K ohms at 10 microamperes and 15 K ohms at 100 microamperes, i.e.,  $R = V/I$ .



To accurately measure the forward voltage to 100 microvolts or better, consideration must be given to the input impedance of the voltage measurement system being used. For example, a digital voltmeter with a ten megohm input impedance will have an effect on the 10 millivolt position for a current of 10 microamperes. For the 100 microampere current source, the loading effect will be seen in the one millivolt position. Therefore, for a calibrated device, readings must be taken with a very high input impedance voltage measurement system. If, however, a sensor is calibrated with a voltmeter of less than infinite impedance, as long as the same system is used, (i.e., the loading is not changed), accurate temperature measurement should be possible.

Insufficient evaluation of and attention to this feature can result in serious temperature measurement errors. For this reason, 10 megohm input impedance DPM's or DVM's at 10 uA diode excitation are not recommended. Fortunately, there is no dearth of DVM's or DPM's with the desired characteristics, i.e., 1 Volt range with 100 or 200% overrange and input in the  $10^9$  to  $10^{10}$  range. Differential voltmeters are also a proper choice.

4. The dynamic impedance of the sensor is approximately 1000 ohms at 10 uA and 100 ohms at 100 uA. This is extremely fortunate since it reduces the requirements on the constant current source by nearly two orders of magnitude over that of the voltage measurement system. For example, a current source regulated to 0.1% will cause a change in the 100 microvolt position.

The required temperature accuracy vs. the instrumentation current regulation and voltmeter resolution is:

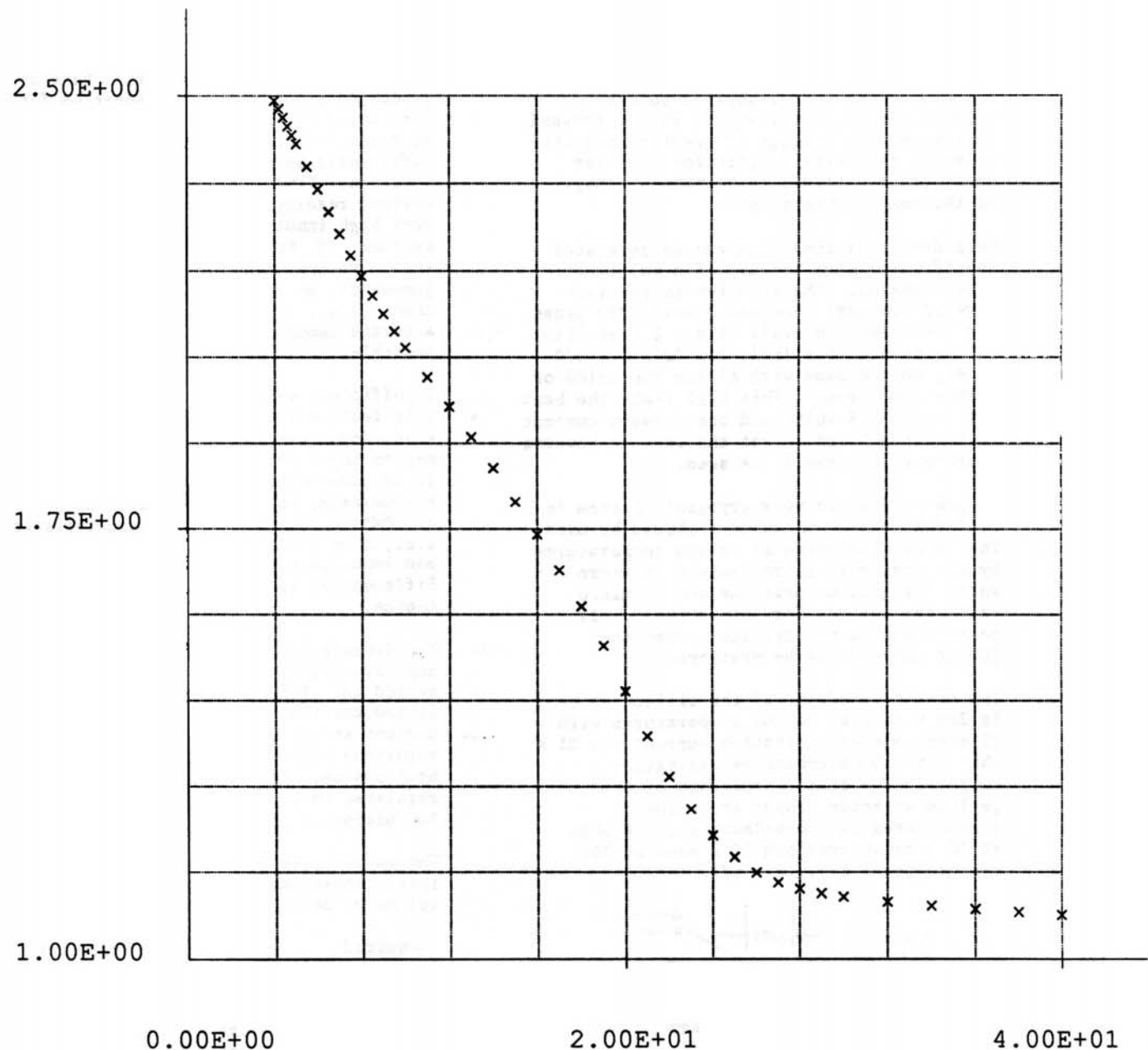
Required Temperature Accuracy	Current Source Resolution	Voltmeter Resolution
1.0 K	5%	1 mV
.1 K	.5%	100 uV
.01 K	.05%	10 uV

## APPENDIX II

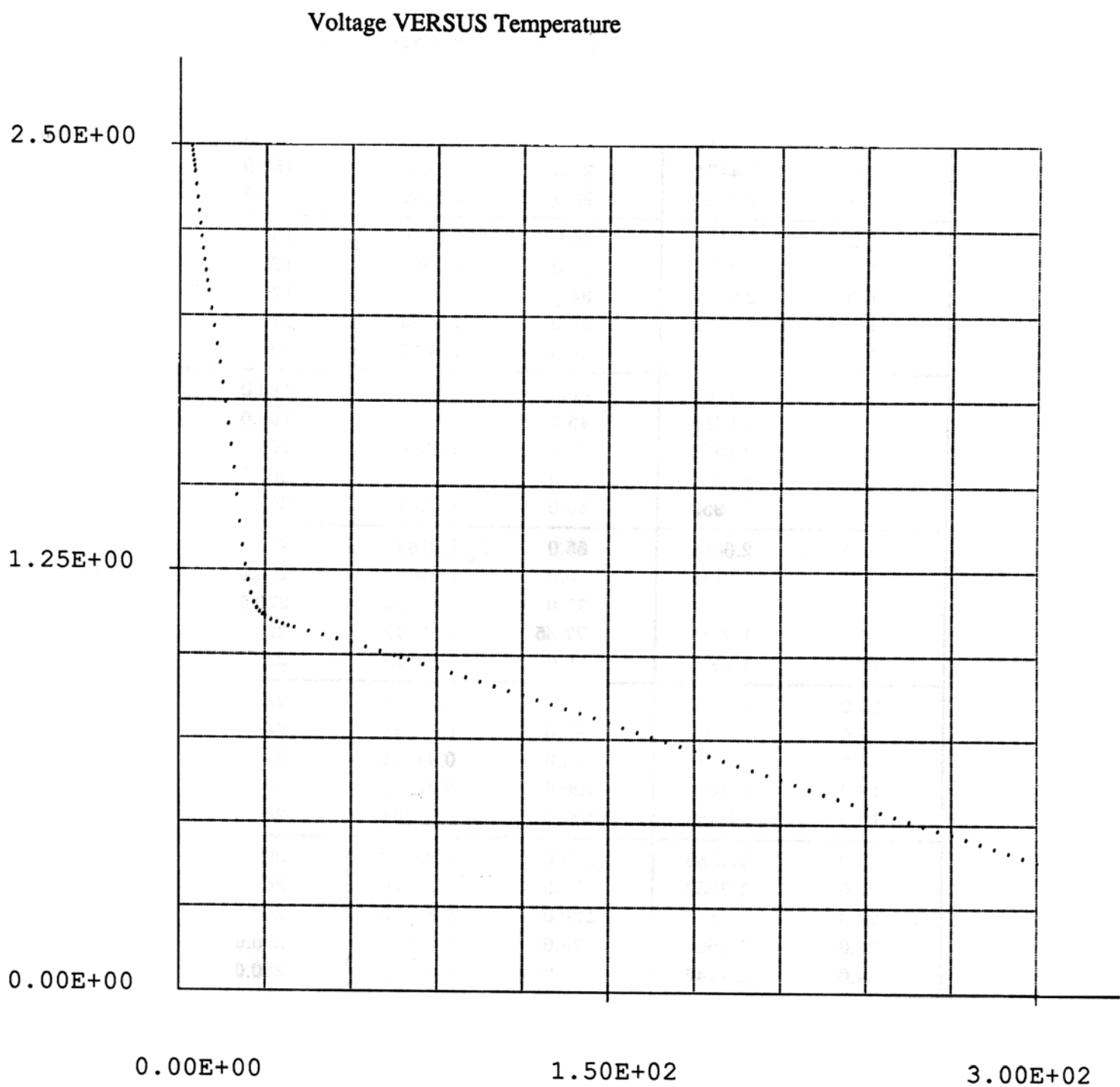
### CALIBRATION CURVES FOR SILICON DIODES

Calibration Curve for Diode (S/N D27807) - Copper Wire Probe (4.2 K → 40 K)

Voltage VERSUS Temperature



# Calibration Curve for Diode (S/N D27807) - Copper Wire Probe (4.2 K → 300 K)

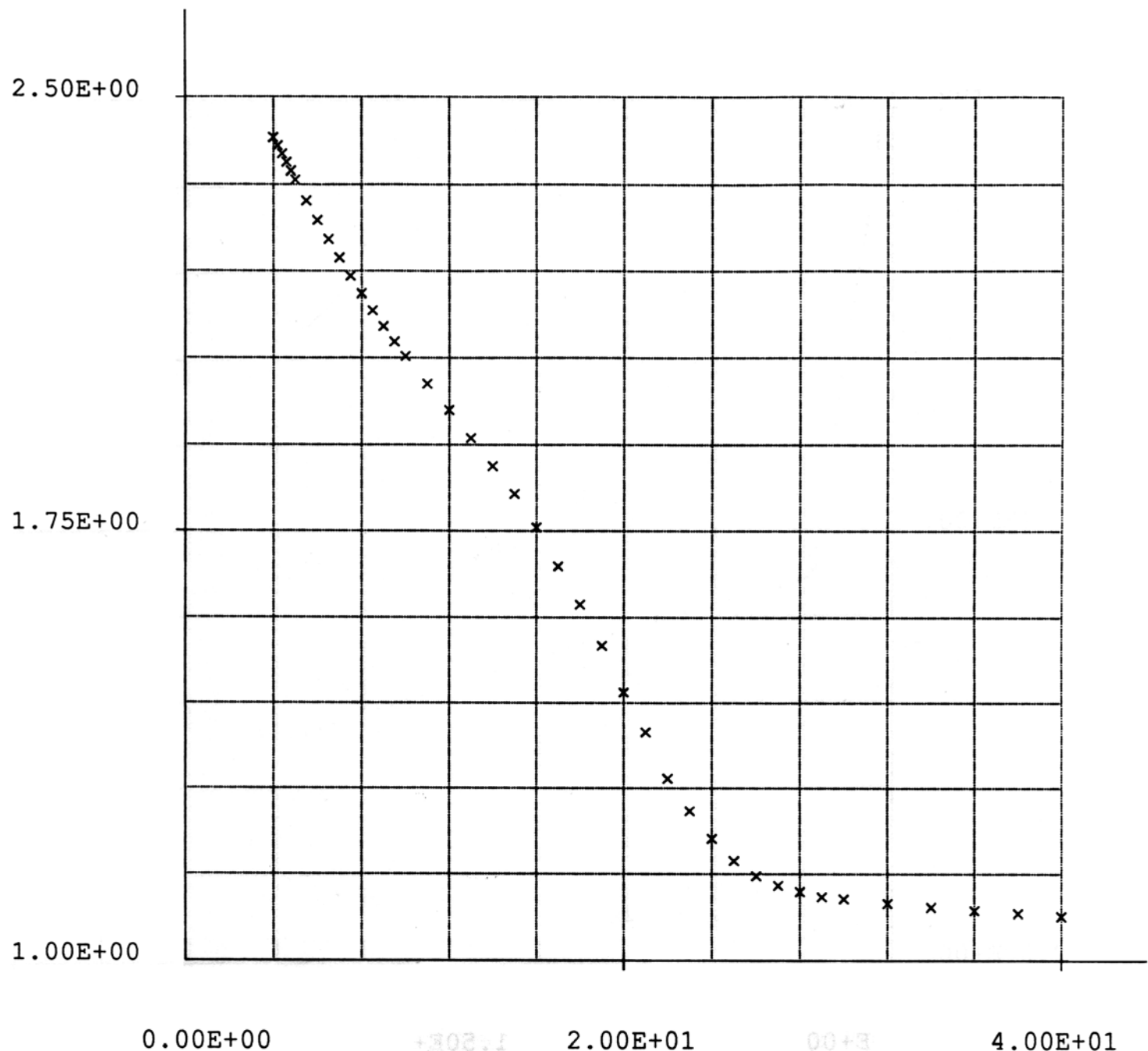


**Calibration Data for Diode (S/N D27807) - Copper Wire Probe**

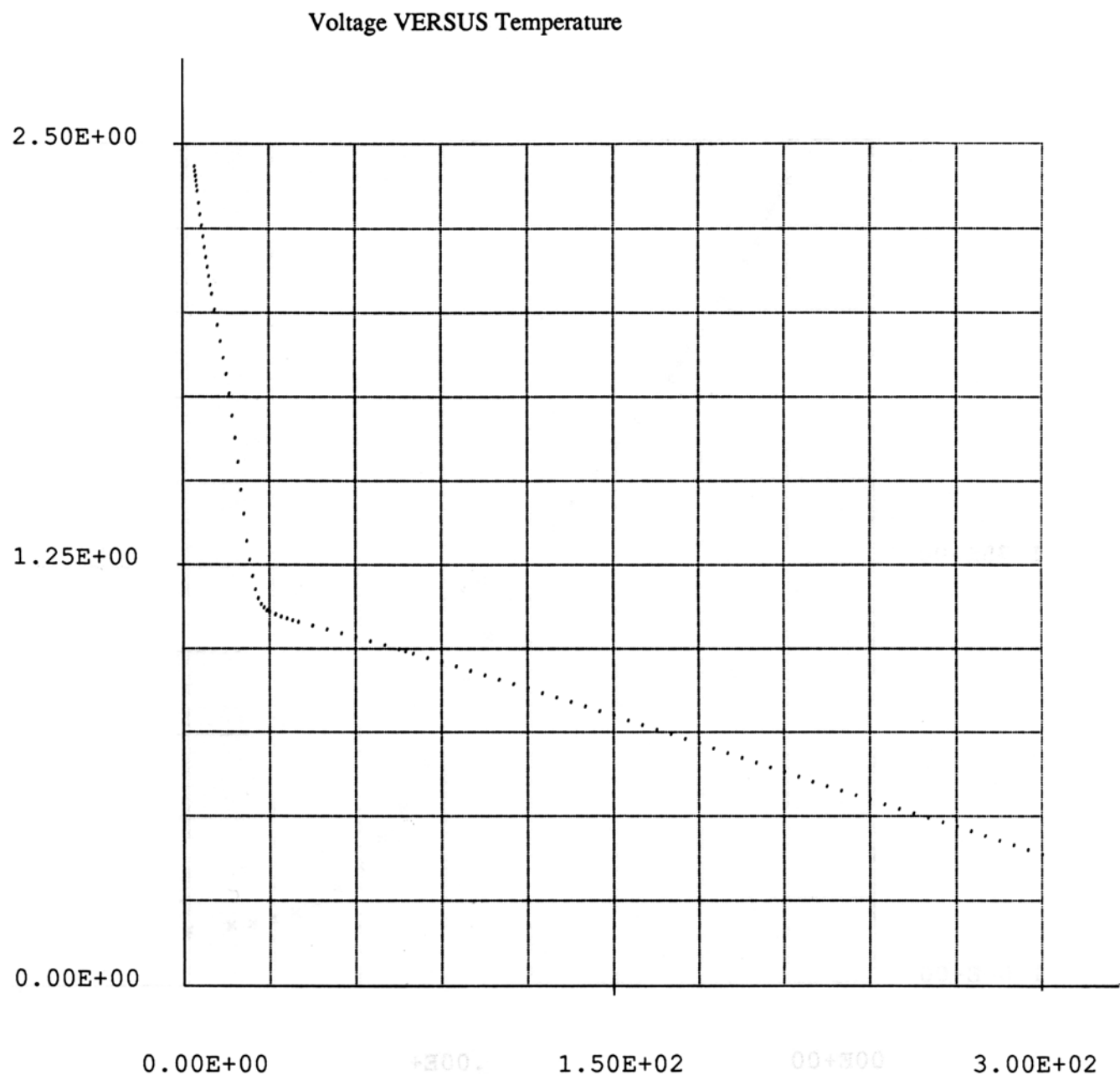
Temperature	Voltage	Temperature	Voltage	Temperature	Voltage
4.0	2.4914	25.0	1.1768	135.0	0.83638
4.2	2.4774	26.0	1.1496	140.0	0.82282
4.4	2.4624	27.0	1.1323	145.0	0.80921
4.6	2.4474	28.0	1.1214	150.0	0.79555
4.8	2.4324	29.0	1.1136	155.0	0.78184
5.0	2.4173	30.0	1.1076	160.0	0.76808
5.5	2.3787	32.0	1.0988	165.0	0.75427
6.0	2.3398	34.0	1.0921	170.0	0.74043
6.5	2.3012	36.0	1.0864	175.0	0.72654
7.0	2.2633	38.0	1.0813	180.0	0.71261
7.5	2.2264	40.0	1.0764	185.0	0.69865
8.0	2.1910	45.0	1.0648	190.0	0.68464
8.5	2.1574	50.0	1.0536	195.0	0.67060
9.0	2.1255	55.0	1.0423	200.0	0.65655
9.5	2.0953	60.0	1.0307	205.0	0.64250
10.0	2.0668	65.0	1.0189	210.0	0.62843
11.0	2.0147	70.0	1.0067	215.0	0.61442
12.0	1.9639	75.0	0.99432	220.0	0.60042
13.0	1.9111	77.35	0.98842	225.0	0.58650
14.0	1.8560	80.0	0.98170	230.0	0.57270
15.0	1.7969	85.0	0.96891	235.0	0.55904
16.0	1.7402	90.0	0.95598	240.0	0.54554
17.0	1.6771	95.0	0.94294	245.0	0.53218
18.0	1.6143	100.0	0.92983	250.0	0.51896
19.0	1.5458	105.0	0.91664	255.0	0.50584
20.0	1.4666	110.0	0.90340	260.0	0.49272
21.0	1.3880	115.0	0.89010	265.0	0.47961
22.0	1.3170	120.0	0.87675	270.0	0.46642
23.0	1.2605	125.0	0.86334	275.0	0.45314
24.0	1.2145	130.0	0.84988	280.0	0.43973
				285.0	0.42620
				290.0	0.41252
				295.0	0.39870
				300.0	0.38476

# Calibration Curve for Diode (S/N D8080) - Lead Wire Probe (4.0 K → 40 K)

Voltage VERSUS Temperature



**Calibration Curve for Diode (S/N D8080) - Lead Wire Probe (4.2 K → 300 K)**

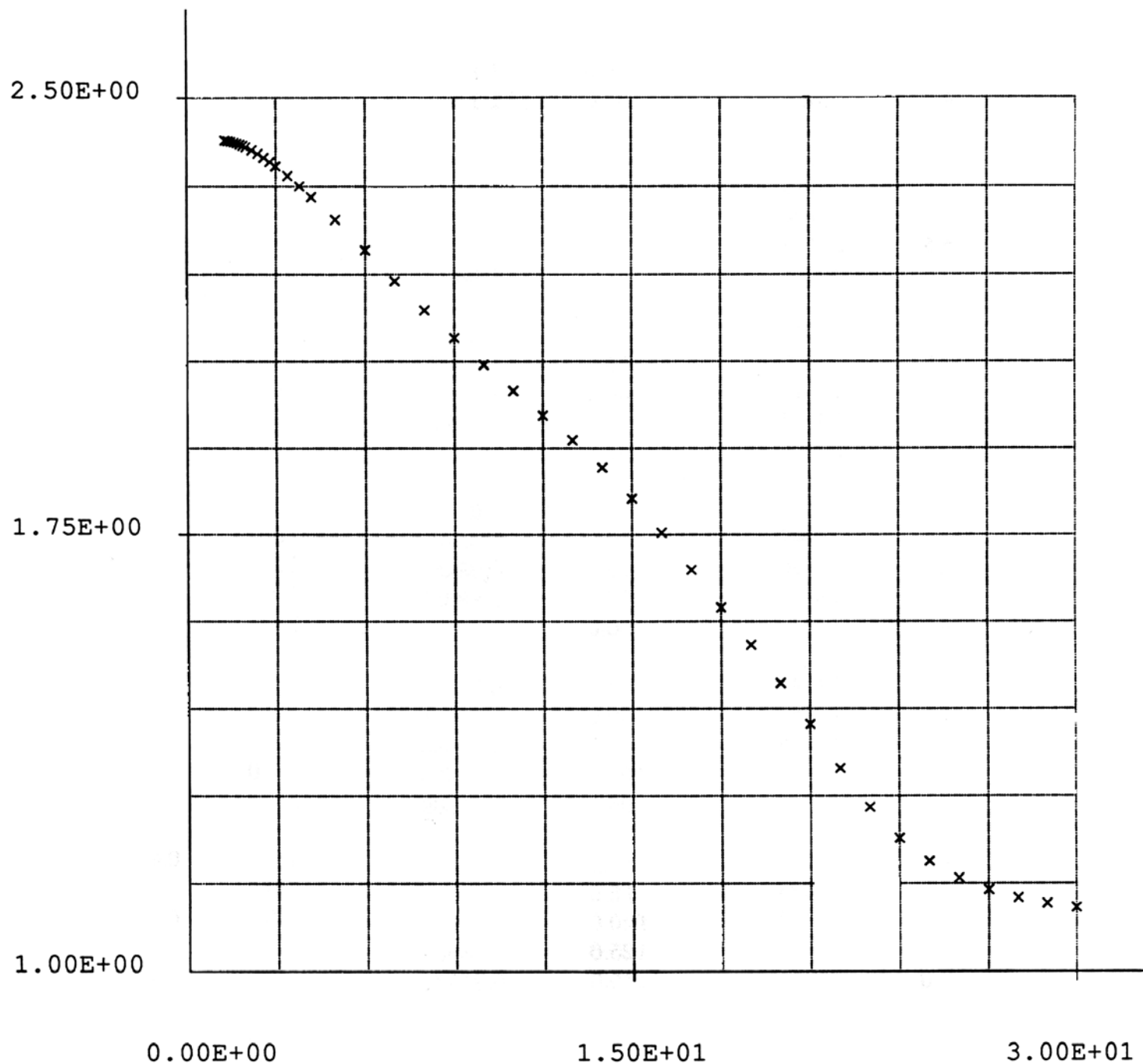


# Calibration Data for Diode (S/N D8080) - Lead Wire Probe

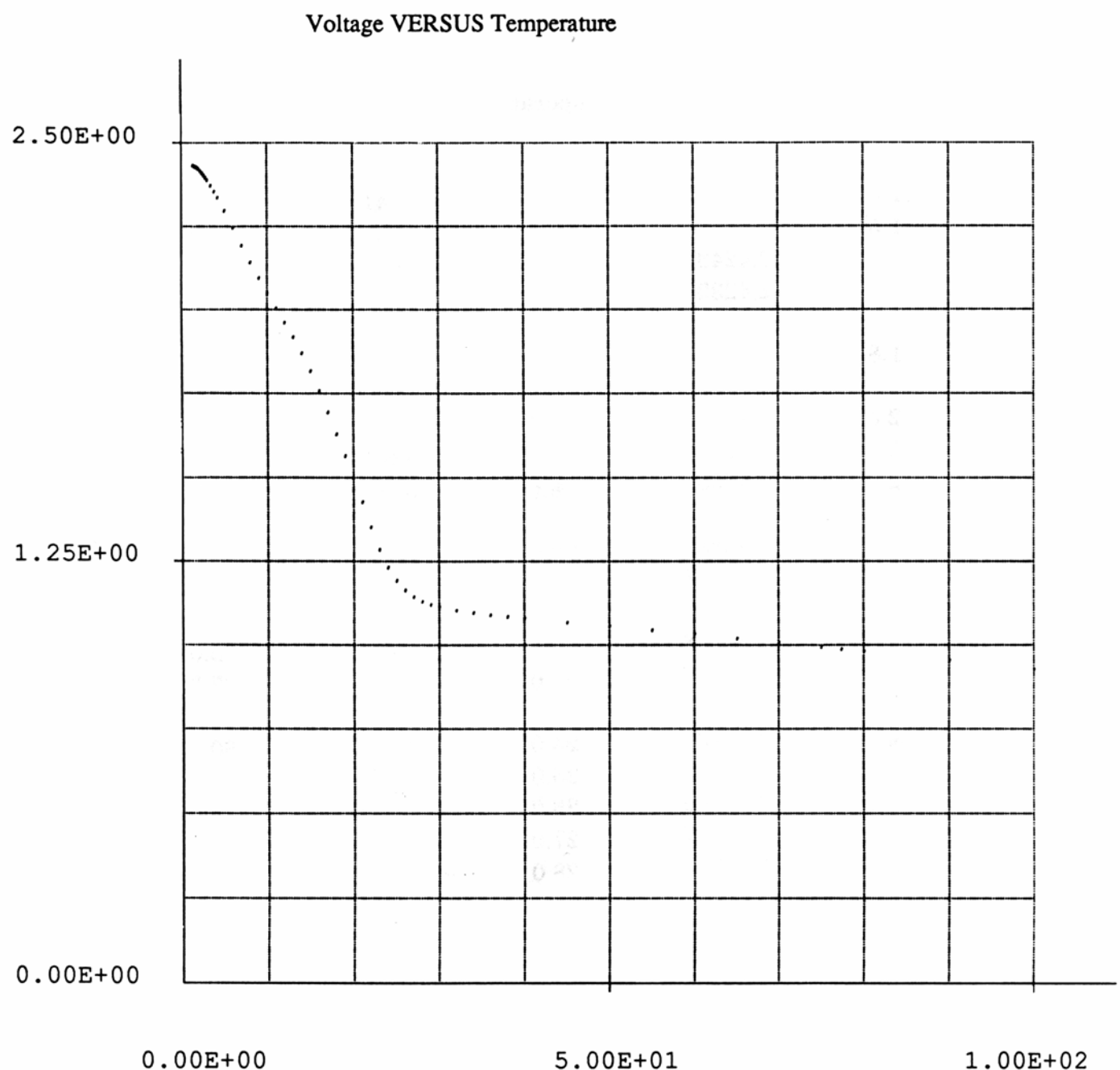
Temperature	Voltage	Temperature	Voltage	Temperature	Voltage
4.0	2.4299	25.0	1.1731	135.0	0.83621
4.2	2.4160	26.0	1.1465	140.0	0.82263
4.4	2.4021	27.0	1.1297	145.0	0.80901
4.6	2.3876	28.0	1.1193	150.0	0.79533
4.8	2.3727	29.0	1.1103	155.0	0.78157
5.0	2.3577	30.0	1.1068	160.0	0.76777
5.5	2.3215	32.0	1.0990	165.0	0.75393
6.0	2.2876	34.0	1.0924	170.0	0.74006
6.5	2.2549	36.0	1.0868	175.0	0.72615
7.0	2.2226	38.0	1.0817	180.0	0.71218
7.5	2.1911	40.0	1.0768	185.0	0.69813
8.0	2.1610	45.0	1.0653	190.0	0.68406
8.5	2.1321	50.0	1.0539	195.0	0.66995
9.0	2.1044	55.0	1.0427	200.0	0.65582
9.5	2.0778	60.0	1.0311	205.0	0.64176
10.0	2.0524	65.0	1.0192	210.0	0.62768
11.0	2.0047	70.0	1.0070	215.0	0.61360
12.0	1.9596	75.0	0.99455	220.0	0.59956
13.0	1.9116	77.35	0.98861	225.0	0.58557
14.0	1.8624	80.0	0.98185	230.0	0.57175
15.0	1.8142	85.0	0.96899	235.0	0.55807
16.0	1.7562	90.0	0.95601	240.0	0.54450
17.0	1.6895	95.0	0.94296	245.0	0.53106
18.0	1.6227	100.0	0.92986	250.0	0.51775
19.0	1.5507	105.0	0.91669	255.0	0.50453
20.0	1.4693	110.0	0.90346	260.0	0.49139
21.0	1.3983	115.0	0.89015	265.0	0.47822
22.0	1.3169	120.0	0.87676	270.0	0.46494
23.0	1.2604	125.0	0.86330	275.0	0.45159
24.0	1.2119	130.0	0.84977	280.0	0.43809
				285.0	0.42443
				290.0	0.41063
				295.0	0.39671
				300.0	0.38267

**Calibration Curve for Diode (S/N D1308) - Gold + 0.07% Iron Wire (1.3 K → 30 K)**

Voltage VERSUS Temperature



**Calibration Curve for Diode (S/N D1308) - Gold + 0.07% Iron Wire (1.3 K → 100 K)**



## Calibration Data for Diode (S/N D1308) - Gold + 0.07% Iron Wire

Temperature	Voltage	Temperature	Voltage	Temperature	Voltage
1.3	2.42813	9.0	2.09012	29.0	1.11635
1.4	2.42730	10.0	2.04411	30.0	1.10948
1.5	2.42620	11.0	1.99949	32.0	1.09956
1.6	2.42484	12.0	1.95662	34.0	1.09209
1.7	2.42322	13.0	1.91360	36.0	1.08568
1.8	2.42136	14.0	1.86598	38.0	1.08016
1.9	2.41926	15.0	1.81255	40.0	1.07519
2.0	2.41692	16.0	1.75340	45.0	1.06345
2.2	2.41163	17.0	1.68946	50.0	1.05188
2.4	2.40558	18.0	1.62420	55.0	1.04002
2.6	2.39889	19.0	1.55969	60.0	1.02784
2.8	2.39166	20.0	1.49370	65.0	1.01531
3.0	2.38397	21.0	1.42265	70.0	1.00249
3.4	2.36748	22.0	1.34780	75.0	0.98943
3.8	2.34983	23.0	1.28097	77.35	0.98322
4.2	2.33130	24.0	1.22772	80.0	0.97619
5.0	2.29221	25.0	1.18825	90.0	0.94934
6.0	2.24059	26.0	1.15978	100.0	0.92215
7.0	2.18817	27.0	1.13931		
8.0	2.13784	28.0	1.12559		

## APPENDIX III

### Chapter 4 of G.T Meaden, Electrical Resistivity of Metals.

#### 4.3. THE PRINCIPAL METHODS OF CALCULATING $\theta_R$ VALUES

We shall consider in this section the four principal methods discussed by Kelly and MacDonald<sup>238</sup> for obtaining, by means of the Grüneisen-Bloch equation,  $\theta_R$  as a function of temperature from measured resistance data. The various methods differ inherently in their degree of reliability and in their relative ease of calculation, both these factors being dependent on the nature of the assumptions made about the constancy or otherwise of  $\kappa$  and  $\theta_R$ .

Methods of Evaluating  $\theta_R$ :

103

In the first method,  $\kappa$  and  $\theta_R$  are initially taken as constants. Then, by comparing the resistances or resistivities  $\rho_{iT_1}$ ,  $\rho_{iT_0}$  at two temperatures  $T_1$ ,  $T_0$ , respectively,  $\kappa/\theta_R^2$  is eliminated on applying equation (4.2). The procedure simply involves finding the value of  $\theta_R$  that satisfies the equation

$$G\left(\frac{\theta_R}{T_1}\right) = \frac{\rho_{iT_1}}{\rho_{iT_0}} \cdot \frac{T_0}{T_1} G\left(\frac{\theta_R}{T_0}\right) \quad (4.8)$$

by means of successive approximation. For convenience,  $T_0$  may be taken as room temperature.

But if we have previous knowledge that over a certain region of temperature the characteristic temperature ( $\theta_0$  at  $T_0$ , say) is practically constant, then equation (4.2) may be used to give instead

$$\left(\frac{T_1}{\theta_1}\right)^2 G\left(\frac{\theta_1}{T_1}\right) = T_1 \rho_{iT_1} \left[ \frac{T_0}{\theta_0^2 \rho_{iT_0}} G\left(\frac{\theta_0}{T_0}\right) \right]$$

From this equation the unknown characteristic temperature  $\theta_1$  at  $T_1$  may be arrived at without any difficulty, since the factor in square brackets is decided at the outset and the right-hand side is easily evaluated afresh at each resistivity point ( $\rho_{iT_1}$ ,  $T_1$ ). To aid the reader in obtaining a rapid solution, we provide in Table IX values of  $(T/\theta_R)^2 G(\theta_R/T)$  as a function of  $\theta_R/T$ .

This method of analysis is more straightforward than the first one and is at the same time more accurate, since from the start it treats  $\theta_R$  as a variable parameter. As in the first method, constancy of  $\kappa$  is assumed, and a minor drawback is that the effect of a suitable choice of reference temperature can occasionally be critical. The following, more elaborate methods which overcome these objections involve a knowledge of the quantity  $(d\rho/dT)/(\rho/T) \equiv (d \log \rho)/(d \log T)$ .

We take logarithms of the Grüneisen-Bloch equation (4.2) and differentiate with respect to  $\log T$ :

$$\begin{aligned} \frac{d \log \rho_i}{d \log T} &= 1 + \frac{d \log G}{d \log T} - 2 \frac{d \log \theta_R}{d \log T} \\ &= + \left[ \frac{d \log G}{d \log(\theta_R/T)} \left( \frac{d \log \theta_R}{d \log T} - 1 \right) \right] - 2 \frac{d \log \theta_R}{d \log T} \end{aligned}$$

Therefore,

$$\frac{d \log \rho_i}{d \log T} = + \left| \frac{d \log G}{d \log(\theta_R/T)} \right| - \frac{d \log \theta_R}{d \log T} \left[ 2 + \left| \frac{d \log G}{d \log(\theta_R/T)} \right| \right] \quad (4.10)$$

Table IX. The Function  $G'(\theta/T) \equiv G(\theta/T)(\theta/T)^2$   
in Terms of  $\theta/T$

$\theta/T$	$G(\theta/T)$	$\theta/T$	$G(\theta/T)$	$\theta/T$	$G(\theta/T)$
0	$\infty$	3.1	0.06378	7.4	0.02293
0.1	99.94	3.2	0.05811	7.6	0.02008
0.2	24.94	3.3	0.05304	7.8	0.021762
0.3	11.06	3.4	0.04845	8.0	0.021548
0.4	6.195	3.5	0.04430	8.2	0.021362
0.5	3.946	3.6	0.04058	8.4	0.021201
0.6	2.723	3.7	0.03718	8.6	0.021062
0.7	1.986	3.8	0.03412	8.8	0.02091
0.8	1.508	3.9	0.03133	9.0	0.020822
0.9	1.180	4.0	0.02880	9.2	0.0207384
1.0	0.9465	4.1	0.02650	9.4	0.020653
1.1	0.7732	4.2	0.02439	9.6	0.0205843
1.2	0.6418	4.3	0.02246	9.8	0.0205258
1.3	0.5395	4.4	0.02070	10.0	0.0204655
1.4	0.4584	4.5	0.01909	10.5	0.0203534
1.5	0.3932	4.6	0.01762	11.0	0.0202708
1.6	0.3400	4.7	0.01628	11.5	0.0202093
1.7	0.2960	4.8	0.01505	12.0	0.0201634
1.8	0.2592	4.9	0.01391	12.5	0.0201285
1.9	0.2282	5.0	0.01287	13	0.0201021
2.0	0.2018	5.2	0.01104	14	0.02006577
2.1	0.1793	5.4	0.009475	15	0.02004357
2.2	0.1598	5.6	0.008155	16	0.02002963
2.3	0.1429	5.8	0.007034	17	0.02001661
2.4	0.1282	6.0	0.006075	18	0.02001463
2.5	0.1153	6.2	0.005258	20	0.02001777
2.6	0.1040	6.4	0.004558	22	0.020014390
2.7	0.09391	6.6	0.003960	24	0.020012604
2.8	0.08502	6.8	0.003445	26	0.020011611
2.9	0.07713	7.0	0.003003	28	0.02001033
3.0	0.07008	7.2	0.002662		

When  $\theta_R$  is constant, this simplifies to

$$\frac{d \log \rho_t}{d \log T} = 1 + \left| \frac{d \log G}{d \log(\theta_R/T)} \right| \quad (4.11)$$

The function on the right-hand side of this last equation is tabulated in terms of  $\theta_R/T$  in Table X. The lower part of the range as far as  $\theta_R/T = 1.6$  has been evaluated by making use of the simple polynomial expansion of  $G(\theta_R/T)$  in terms of  $\theta_R/T$  given by Gruneisen.<sup>183</sup> The remainder of the table up to  $\theta_R/T = 15.0$  we have solved using a graphic method.<sup>303</sup> Henry and Schroeder<sup>211</sup> have calculated the above function at intervals of 0.04 between  $\theta_R/T = 0.04$  and 1.80.

Table X. Values of  $1 + [(d \log G)/(d \log(\theta_R/T))]$   
as a Function of  $\theta_R/T$

$\theta_R/T$	$+ \left  \frac{d \log G}{d \log(\theta_R/T)} \right $	$\theta_R/T$	$+ \left  \frac{d \log G}{d \log(\theta_R/T)} \right $	$\theta_R/T$	$+ \left  \frac{d \log G}{d \log(\theta_R/T)} \right $
0.1	1.00111	0.2	1.00444	0.3	1.00998
0.4	0.4	0.4	0.4	0.5	0.5
0.7	0.6	0.6	0.6	0.7	0.7
1.0	0.7	0.7	0.7	0.8	0.8
1.3	0.8	0.8	0.8	0.9	0.9
1.6	0.9	0.9	0.9	1.0	1.0
2.0	1.1	1.1	1.1	1.1	1.1
2.4	1.2	1.2	1.2	1.2	1.2
2.8	1.3	1.3	1.3	1.3	1.3
3.2	1.4	1.4	1.4	1.4	1.4
3.6	1.5	1.5	1.5	1.5	1.5
4.0	1.6	1.6	1.6	1.6	1.6
4.4	1.7	1.7	1.7	1.7	1.7
4.8	1.8	1.8	1.8	1.8	1.8
5.2	1.9	1.9	1.9	1.9	1.9
5.6	2.0	2.0	2.0	2.0	2.0
6.0	2.1	2.1	2.1	2.1	2.1
6.4	2.2	2.2	2.2	2.2	2.2
6.8	2.3	2.3	2.3	2.3	2.3
7.2	2.4	2.4	2.4	2.4	2.4
7.6	2.5	2.5	2.5	2.5	2.5
8.0	2.6	2.6	2.6	2.6	2.6
8.4	2.7	2.7	2.7	2.7	2.7
8.8	2.8	2.8	2.8	2.8	2.8
9.2	2.9	2.9	2.9	2.9	2.9
9.6	3.0	3.0	3.0	3.0	3.0

With this table,  $\theta_R/T$  can be deduced directly at any temperature by means of equation (4.11), since  $(d \log \rho_t)/(d \log T)$  is given by the experimental observations. This is the third method of Kelly and MacDonald. It is not exact because the derivation of equation (4.11) itself assumes a constant  $\theta_R$ . Its purpose is to obtain a preliminary, though rough,  $\theta_R-T$  graph before passing on to the more precise equation (4.10); the procedure with equation (4.10) is to begin in a region in which  $\theta_R$  has already been discovered to be virtually constant. Then the correction term in this equation is small, and accurate  $\theta_R$  values may be calculated quickly by successive approximation. The success of these two methods depends on good, closely spaced experimental results in order that  $(d \rho_t/dT)(\rho_t)$  may be enumerated with sufficient precision.

The relative merits of all four methods may be compared by referring to Fig. 33, in which  $\theta_R-T$  curves derived from the same set of

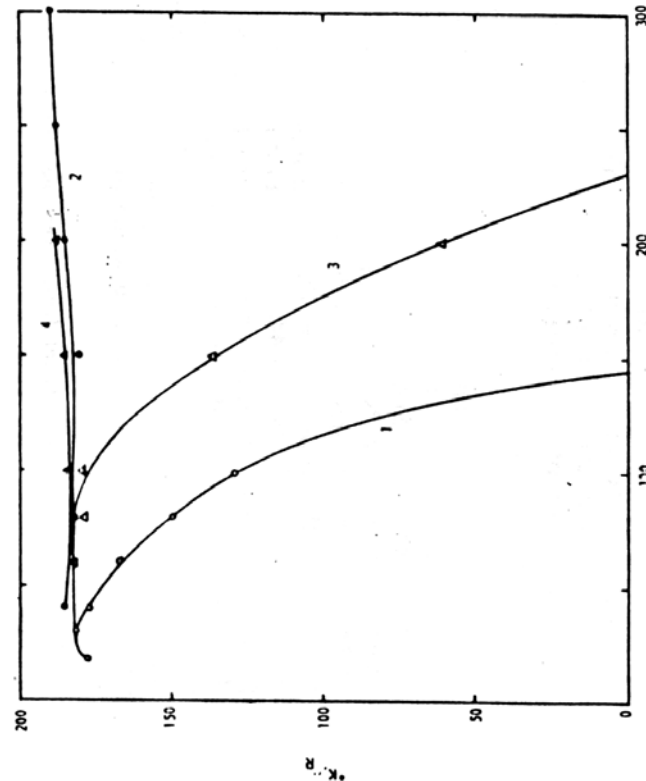


Fig. 33.  $\theta_K$  for Na evaluated by four different methods. Experimental data of MacDonald, which were corrected for thermal expansion, were used (Kelly<sup>237</sup>).

experimental data are given. In this example by Kelly<sup>237</sup> based on MacDonald's experimental results, the first and third methods do not work out well. The huge temperature coefficients of  $\theta_K$  arise chiefly because the basic formulas assume constant  $\theta_K$  values. Naturally, then, the methods prove to be correct at only the lower temperatures where  $\theta_K$  really is almost constant. The computations made by employing methods 2 and 4 both began in these regions. That they both result in rather similar temperature dependences implies that  $\kappa$ , the electron-phonon interaction parameter, is in fact constant over the temperature range considered. In such a case, method 2 is to be recommended on account of its greater ease of manipulation.

In analyzing the data for Fig. 33, Kelly also took into consideration another factor that is particularly important in the highly compressible alkali metals. He corrected for the dependence of the electrical resistivity on thermal expansion. This was also done by Dugdale and

Gugan for the alkali metals of Fig. 31, whose  $\theta_K$  values were computed according to the fourth method above. We have indicated before that experimental observations are normally taken under conditions of constant pressure, while theory always relates to the resistivity at constant volume. The density corrections necessary because of temperature changes can only be accurately applied if the pressure coefficient of resistivity is known. Fortunately, such corrections are small for most metals and are usually neglected. They are, however, very large for some of the alkalis, notably K, and the corrections to be made have been considered by Kelly<sup>237</sup> (also for the noble metals), Dugdale and Gugan,<sup>139</sup> and Meixner.<sup>314</sup>

#### 4.4. RULE-OF-THUMB METHOD FOR $\theta_K$

This is a simple and rough and ready method that gives only a single  $\theta_K$  value for a metal but which can be worked out almost instantly and sometimes even by mental arithmetic. More often than not, the accuracy is to within 10%.

We make use of equation (4.5) and always take  $T_I = 20$  and  $T_h = 295^{\circ}\text{K}$ . We then obtain

$$\theta_K = 48.20 \left( \frac{\rho_{T=295}}{\rho_{T=20}} \right)^{1/4} \quad (4.12)$$

as a practical and easily remembered formula. Resistances at just three temperatures need to be known or measured in order that it may be solved, namely, the resistances at room temperature and at the hydrogen and helium points. The result achieved is a single value that represents  $\theta_K$  for the metal over a wide temperature range below room temperature. The formula must be used with care, and the conditions under which it is valid recognized from the beginning.

First, equation (4.5) itself cannot be expected to be correct (or almost correct) unless  $\rho_{\text{lit}}$  is taken in a region where  $\rho_{\text{lit}} \propto T^n$  with  $n = 4.5$  to 5.5.  $T_I = 20^{\circ}\text{K}$  was chosen not only because it is the hydrogen point and because  $\rho_{T=20}$  is sufficiently large in magnitude to be measured with adequate precision but also because in a number of metals this temperature is located in the  $T^5$  region ( $T_I < \theta/5$  to  $\theta/10$ ). Obviously, the formula leads to  $\theta_K$  values which are too small in the cases of transition metals, rare earths, and very impure metals, where other temperature-dependent scattering mechanisms partially or wholly conceal the  $T^5$  lattice scattering term to which equations (4.5) and (4.12) relate. We now append a list of  $\theta_K$  values calculated by equation (4.12) for nontransition metals using data abstracted from Table II. The reader can judge for himself the extent of the agreement

between these albeit rough  $\theta_R$  figures and the high-temperature  $\theta_D$  and  $\theta_R$  values of Table VIII. The list is: Li 241\*; Na 189,\* Mg 229,\* Al 396; K 130,\* Cu 327, Zn 157(177†); Ga 173, As 152; Rb 107,\* Sr 125, Ag 219, Cd 132, In 131, Sn 156, Sb 152; Cs 99,\* Ba 130, Au 176, Hg 106, Ti 120, Pb 119, and Bi 102°K. It should be recalled that these  $\theta_R$  values are appropriate for the range up to 295°K, which is not always the same as the range between  $T \sim \theta/2$  and  $\theta$ . If we therefore make comparisons with the appropriate  $\theta_R$  wherever possible, otherwise with  $\theta_D$ , we find differences greater than 10% only in Li, Mg, K, Ga(?), As, Rb, and Cs. In these metals there is either no  $T_3$  region at all or else it appears only at temperatures well below 20°K.

The latter would certainly be the case in Rb and Cs, which have very low  $\theta_D$ . The use of a  $T_3$  lower than 20°K would obviously produce more satisfactory results all round, but accurate data for  $\rho_i$  at 10°K or so are much scarcer in the literature and more difficult to obtain in practice than are data at the hydrogen point. But if we recalculate  $\theta_R$  values for K, Rb, and Cs using  $T_3 = 8^\circ\text{K}$ , for which accurate figures are available,<sup>139,142</sup> we obtain for the respective  $\theta_R$  values for these metals 82, 57, and 47°K. These figures compare quite well with mean  $\theta_R$  and  $\theta_D$  for the temperature range below room temperature.

Of the transition elements, satisfactory agreement is found for Ti 328, Mo 372,‡ Ru 395,‡ Rh 346, Hf 200, Re 279, Os 335,‡ and Ir 272. These are transition metals for which White and Woods<sup>140</sup> give temperature exponents at low temperatures that lie in the range 4.6 to 5.3. For other transition metals, equation (4.12) gives  $\theta_R$  values that are between 10 and 35% smaller than the  $\theta_R$  and  $\theta_D$  figures of Table VIII for the reasons explained above. With data from Table II, quite reasonable  $\theta_R$  values are obtained for the actinide metals, namely, Th 144, U 128 and 121, and Np 135 (see Table VIII). Semenenko and Sudovitsov<sup>95</sup> have analyzed their 14 to 20°K resistivity data on Fe, Ni, and Pt into separate  $T^2$  and  $T^5$  terms. If we make use of their figures for  $\rho_{120}$  (based on the  $T^5$  term) and  $\rho_{1273}$  and then employ the formula  $\theta_R = 49.14 (\rho_{1273}/\rho_{120})^{1/4}$ , we discover that for Fe  $\theta_R = 460$ , for Ni it is 440, and for Pt it is 217°K. These are all perfectly acceptable values compared to the  $\theta_D$  results. Obviously, this approximate method is best used when a  $(\rho_i, T_3)$  point is available from a region where the  $T^5$  law is valid; in those cases where other scattering terms are present in the  $T_H$  region, the lattice term should be separated if possible and used alone in equation (4.12). Such a

procedure requires experimental measurements of very high precision if an accurate plot of  $\rho_i T^{-2}$  against  $T^3$  is to be obtained, but while such studies are important for theoretical purposes, they are not in keeping with the spirit of the rough and ready  $\theta_R$  rule.

Summarizing, we are able to say that equation (4.2), or any of its related equations, provides a rapid means of estimating a representative  $\theta_R$  value for a metal (with the admitted limitations discussed above) in a convenient and practical manner requiring a minimum of experimental data, since in principle only the relative ideal resistances at 20°K and room temperature are required.

\* Readings corrected to constant density were used.<sup>139, 142</sup>

† With data from ref. 42.

‡  $T_3$  was taken as 25 K since ref. M10 had no data for 20 K. The formula then becomes  $\theta_R = 63.70 (\rho_{1273}/\rho_{120})^{1/4}$ .

## APPENDIX IV

### Effect That Magnetic Exchange Interaction Has on the Specific Heat of Magnetic Alloys

Taken From: H.J. Zeiger and G.W. Pratt, Magnetic Interactions in Solids.

522

INDIRECT INTERACTIONS IN METALS

In another series of studies [25], it has been found that the addition of other rare earth ions to a dilute alloy of Gd in Pd produces an additional line shift of the Gd resonance, consistent with an apparent long range polarization of the conduction electrons by the rare earth ions. The additional shift is too large to be given by an ordinary RKKY interaction. Proposed explanations involve modifications of the RKKY model, which will be discussed in Section 8.7.

#### 8.5.3. Specific heat of dilute magnetic alloys

At low temperatures, dilute magnetic alloys show remarkable properties, which are undoubtedly related to the long range indirect exchange interaction between the solute ions, produced by conduction electron polarization. Since the early studies of the specific heats of dilute alloys of Mn in Cu [26], [27], an enormous body of theoretical and experimental work on the properties of dilute magnetic alloys has been produced [28]. Much still remains to be understood concerning such systems, and a brief discussion of developments in the field is deferred to Section 8.7. However, we will consider here a simple heuristic model of dilute alloys of Mn in Cu, which provides a useful starting point for understanding the specific heat and other properties of these alloys.

Dilute alloys of Mn in Cu ( $\sim 0.1\text{--}10$  per cent) show a broad transition region with decreasing temperature, going over to a low temperature state with striking properties. Among these are a magnetic impurity contribution to the specific heat which is relatively large, linear in temperature, and independent of impurity concentration. Because of the random distribution of magnetic impurities, these alloys have been termed 'magnetic glasses' [29]. Marshall [28] has presented a simple physical picture to explain these properties, and Brout and Klein [30], [31], and Liu [32] performed detailed self-consistent studies of the model, which confirm Marshall's general picture.

In Marshall's model, the impurities are assumed to have spin  $\frac{1}{2}$ , and each impurity experiences an effective field  $H$  along some axis, due to its indirect exchange interaction with neighbouring impurities. Referring to eqns (3.74) and (3.74b), the thermal average moment of a single spin in the field  $H$  is,

$$m = \mu \tanh(\mu H/kT). \quad (8.50)$$

The thermal average energy of a moment is,

$$\mathcal{E} = -\mu H \tanh(\mu H/kT), \quad (8.51)$$

and averaging over the probability distribution  $p(H, T)$ , of finding a particular value of  $H$  at an impurity site at a given temperature, the total thermal energy per unit volume of the moments is,

$$\mathcal{E}(T) = -\frac{n}{2} c \int_{-\infty}^{\infty} \mu H \tanh\left(\frac{\mu H}{kT}\right) p(H, T) dH. \quad (8.52)$$

The factor of  $\frac{1}{2}$  is due to the fact that  $H$  is an effective indirect exchange field due to all the other moments, so that without the  $\frac{1}{2}$ , we would be counting each spin's effect twice.  $n$  is the number of atoms per unit volume of the crystal, and  $c$  is the fractional concentration of impurities. Differentiating (8.52) with respect to  $T$ , the magnetic specific heat becomes,

$$\begin{aligned} C_M(T) &= \frac{n}{2} c \int_{-\infty}^{\infty} \frac{(\mu H)^2}{kT^2} \operatorname{sech}^2\left(\frac{\mu H}{kT}\right) p(H, T) dH \\ &\quad - \frac{nc}{2} \int_{-\infty}^{\infty} \mu H \tanh\left(\frac{\mu H}{kT}\right) \frac{\partial p(H, T)}{\partial T} dH. \end{aligned} \quad (8.53)$$

Marshall next argues that  $p(H, T)$  will be of the general form shown in Fig. 8.6, having a spread given roughly by  $h(T) \equiv \int_{-\infty}^{\infty} dH |H| p(H, T)$ , and a height at  $H = 0$  of  $\sim 1/h(T)$ . The contribution to the specific heat at low temperatures will come mainly from those spins for which  $H \sim 0$ . On the other hand, at low temperatures, most of the spins will see fields  $H$  such that  $\mu H \gg kT$ , and will be rigidly aligned, making  $h(T)$  temperature insensitive. Assuming then, that the variation of  $p$  with  $T$  is not large at low temperatures, eqn (8.53) becomes,

$$\begin{aligned} C_M(T) &\cong \frac{n}{2} cp(0, 0) \int_{-\infty}^{\infty} \frac{(\mu H)^2}{kT^2} \operatorname{sech}^2\left(\frac{\mu H}{kT}\right) dH \\ &\cong \frac{n}{2} cp(0, 0) \frac{k^2 T}{\mu} \int_{-\infty}^{\infty} x^2 \operatorname{sech}^2 x dx \\ &\cong \frac{n}{2h(0)} \frac{k^2}{\mu} c T \int_{-\infty}^{\infty} x^2 \operatorname{sech}^2 x dx. \end{aligned} \quad (8.54)$$

Now, if the impurity moments interact via an indirect exchange interaction of the RKKY form then, referring to eqn (8.41),  $h(0)$  must be roughly of the form,

$$h(0) \sim \text{const} \left\langle \left( \frac{1}{R_{ab}^3} \right) \right\rangle \sim \text{const. } n.c. \quad (8.55)$$

Combining eqns (8.54) and (8.55),

$$C_M(T) \cong \frac{k^2}{2 \cdot \text{const. } \mu} T \int_{-\infty}^{\infty} x^2 \operatorname{sech}^2 x dx, \quad (8.56)$$

which is linear in  $T$ , and independent of concentration, as observed experimentally.

## APPENDIX V

REVIEWS OF MODERN PHYSICS

VOLUME 40, NUMBER 2

APRIL 1968

# Localized Magnetic Impurity States In Metals: Some Experimental Relationships\*

M. D. DAYBELL,† W. A. STEYERT

*Los Alamos Scientific Laboratory, University of California, Los Alamos, New Mexico*

Evidence is reviewed which demonstrates that the recently observed low-temperature electron state arising from the Kondo effect in metals containing small numbers of transition element impurities is present over a much wider temperature range than is generally appreciated. The possibility that this state forms a link between magnetic and nonmagnetic impurity states in metals as suggested by Schrieffer is discussed.

## INTRODUCTION

Recent experimental observations of a new electron state in metals containing a small number of magnetic impurity ions<sup>1-4</sup> have confirmed theoretical predictions<sup>5-20</sup> that a "quasi-bound state" should be formed between the magnetic moment of a localized impurity and the average moment of the itinerant electrons in its vicinity. This state is analogous in some ways to the Cooper pair in superconductors. Evidence based partly on very recent data and partly on a review (in the light of recent theoretical developments) of the earlier literature,<sup>21</sup> shows that the occurrence of the quasi-bound state is much more widespread than is generally realized, and is not strictly a low-temperature phenomenon. Since the temperature  $T_K$  below which this state exists depends exponentially on the exchange constant  $J$  between the impurity spin and that of the

conduction electrons, the possibility that small changes in  $J$  can vary  $T_K$  from millidegrees to thousands of degrees is not at all unlikely, as has been pointed out recently by Schrieffer.<sup>12</sup>

In the few matrix-impurity systems that have been well-studied experimentally, it is possible to formulate rules which predict the occurrence of quasi-bound states in some alloys for which data are not yet available. Some justification for these rules may be obtained from a slight extension of existing theoretical models. Various fruitful directions for future experimental investigations in solid and liquid metals are discussed.

Section I is a brief noncritical review of some of the theoretical concepts relevant to the experimental observations. Current theoretical activity in this field is quite high, amounting to a few papers a month, and no attempt has been made to cite all the available work although many references to the original literature are given.<sup>22</sup> In Sec. II, the detailed behavior predicted by some of the theories for various experimentally measurable quantities is examined. A description is given of the way in which this information is used to obtain values of certain characteristic temperatures  $T_c$  which form estimates of  $T_K$  for the various alloys for which data are available. The results of this analysis are presented in a series of figures and tables. One way of interpreting the highly systematic variation of  $T_K$  with position of the impurity in the periodic table, based on the recent conjectures of Schrieffer,<sup>12</sup> is discussed in Sec. III. The concluding section deals with other questions which the results of the present review may help to resolve, as well as raising a few new ones.

## I. THEORETICAL CONCEPTS

If a dilute alloy M-I is formed by dissolving a small number of first-row transition-metal atoms I in a metallic matrix M, it is often found that the impurity has a net moment arising from the d-shell valence electrons of the impurity. This localized magnetic impurity state has dramatic effects on many of the electronic properties of the alloy. Many of these effects are discussed in a later section, but for the present attention is confined to the properties of the state itself.

Some time ago, Friedel gave a phenomenological

\* An extensive review by G. J. Van den Berg, in *Progress in Low Temperature Physics*, C. J. Gorter, Ed. (North-Holland Publ. Co., Amsterdam, 1964), Vol. IV, p. 194, discusses the situation before the development of the concept of the quasi-bound state.

† The situation up to 1965 is reviewed by M. Baily, *Advan. Phys.* 15, 179 (1966).

explanation of the local moment in terms of the concept of the "virtual bound state."<sup>23</sup> It was pointed out that the *d* orbitals of the 3*d*-shell valence electrons of a transition-metal atom dissolved in a metal would retain much of their localized character, even when they are embedded in the conduction band of the host material. The effect of the conduction band states on an electron in this localized state could be allowed for, at least to first order, by simply letting the atomic *d* level be broadened and shifted in energy from its unperturbed value. This shift would be just enough to keep the ionic charge on the impurity equal to that of the host. An electron could not be permanently bound in this virtual state, since it would be able to leak out into conduction band states having similar energies, but most of its wave function would be localized very near to the impurity if the broadening of the virtual level were small.

Another way of treating the interaction of the conduction electrons with the impurity is to reduce the system to an equivalent scattering problem.<sup>23,24</sup> In this picture, the impurity first gives up all its *s* and *d* valence electrons to the conduction band of the host, creating a strong localized attractive Coulomb potential well which is almost deep enough to have bound *d* states for every *d* electron given up. Enhancement of the conduction electron wave functions near the impurity by the resonances that then exist in the *d*-wave part of their scattering cross sections at electron energies near those of the vacated *d* levels is strong enough to screen out most of the excess positive charge that was left on the impurity when its valence electrons were removed.

To explain the presence of a net magnetization on an impurity, Friedel pointed out that the exchange and correlation effects responsible for Hund's rule (which for a free atom determines the net spin of an atomic *d* shell containing more than one electron) would operate to separate the energy of the virtual bound state for spin-up electrons from that for those of opposite spin. When the virtual level is narrow enough for this to occur, a net magnetic moment will result in cases where the number of spin-up levels exceeds the number of spin-down levels for energies less than the Fermi energy  $E_F$ . Using the requirement of electrical neutrality to estimate the occupation numbers of the virtual levels, Blandin and Friedel<sup>23</sup> were able to construct a table predicting whether or not a localized moment would occur in some typical alloys. A recent version<sup>24</sup> is given in Table I.

To put these ideas on a more quantitative basis,

TABLE I. (After Friedel.) Dilute alloy systems for which localized moments are known to occur are represented by +; a — implies that no moment occurs (under the earlier interpretations).

	Fermi energy increases →						
	PdH	Au	Ag	Cu	Mg	Zn	Al
Sc							
Ti		—					—
V		+					—
Cr	+	+	+	+	+	+	—
Mn	+	+	+	+	+	+	—
Fe	+	+		+	+	—	—
Co	?	+		?			—
Ni	—	—	—				—

Anderson solved the following simple model in the Hartree-Fock approximation, for temperature  $T = 0^\circ\text{K}$ .<sup>25-27</sup> Assume a localized moment exists, and can be represented by a single *d*-orbital level whose energy is a distance  $\epsilon_d$  below the Fermi level, so that it is occupied by an electron of say, spin-up. A spin-down electron attempting to occupy the same level will see the full repulsive Coulomb interaction  $U$  between it and the *d* electron already on the impurity, and so could only occupy a level whose energy is  $-\epsilon_d + U$ , which must be empty by our assumption that a moment exists, and hence lie above the Fermi level. Now, as before, the conduction electrons can, through the *s-d* mixing interaction,  $V_{kd}$ , mix with the electron in the localized level and cause that level (and the empty level above the Fermi energy) to be broadened and shifted. The broadening of the spin-up level pushes the high-energy tail of its energy distribution above the Fermi level so that it can be partially empty, reducing the average number of localized spin-up electrons to less than one. At the same time, the broadening of the spin-down state allows it to become partially filled. But this decreases the effect of the Coulomb interaction,  $U$ , and allows the spin-up and spin-down levels to become closer together in energy, so that if the *s-d* interaction is too strong, the configuration becomes unstable, the state collapses to two degenerate levels, and no moment appears. Later work<sup>14,28-32</sup> (taking correlations beyond the HF approximation into account) in fact suggests that only in the case when the spin-up state is nearly always occupied and the spin-down state nearly always empty can a local moment exist. In this situation, unless the virtual level is quite narrow, the two states must be located approximately symmetrically with respect to the Fermi level.

<sup>23</sup> P. W. Anderson, Phys. Rev. 124, 41 (1961); P. W. Anderson and A. M. Clogston, Bull. Am. Phys. Soc. 6, 124 (1961).

<sup>24</sup> C. Kittel, *Quantum Theory of Solids* (John Wiley & Sons, Inc., New York, 1963), p. 338.

<sup>25</sup> P. A. Wolff, Phys. Rev. 124, 1030 (1961).

<sup>26</sup> J. R. Schrieffer and D. C. Mattis, Phys. Rev. 140, A1412 (1965).

<sup>27</sup> B. Kjöllerström, D. J. Scalapino, and J. R. Schrieffer, Phys. Rev. 148, 665 (1966).

<sup>28</sup> J. R. Schrieffer and P. A. Wolff, Phys. Rev. 149, 491 (1966).

<sup>29</sup> G. Kemeny, Phys. Rev. 150, 459 (1966).

<sup>30</sup> A. C. Hewson, Phys. Rev. 144, 420 (1966).

<sup>23</sup> P. De Faget de Casteljau and J. Friedel, J. Phys. Radium 17, 27 (1956); J. Friedel, Can. J. Phys. 34, 1190 (1956); J. Friedel, J. Phys. Radium 19, 573 (1958); A. Blandin and J. Friedel, J. Phys. Radium 20, 160 (1959).

<sup>24</sup> See, for example, E. Daniel and J. Friedel, in *Proceedings of the 9th International Conference on Low Temperature Physics*, J. G. Daunt, D. O. Edwards, F. J. Milford, and M. Yaqub, Eds. (Plenum Press, New York, 1965), p. 933 (Part B).

The same  $s-d$  interaction which shifts the level of the localized spin-up state pulls the energy of the spin-down conduction electron states down into the Fermi sea and pushes the spin-up conduction electron states above it, resulting in a net polarization of the conduction electrons near the impurity. This polarization is antiparallel to that of the  $d$  electron on the impurity,<sup>12,25,30,33</sup> resulting in an effective antiferromagnetic exchange interaction (see below). Its value depends on the strength of the  $s-d$  interaction.

This model has been generalized<sup>12,25,32,34,35</sup> to apply to the more realistic case where there are many degenerate  $d$  levels present, although, for simplicity, the orbital angular momentum has usually been assumed to be completely quenched so that the total angular momentum on the impurity becomes just the net spin angular momentum of these localized  $d$  electrons. The Hamiltonian for the single  $d$ -orbital Anderson model can be expressed as

$$H = H_{\text{cond}} + H_{\text{imp}} + H_{kd}, \quad (1)$$

where  $H_{\text{cond}}$  is the unperturbed conduction electron Hamiltonian of the pure matrix metal,  $H_{\text{imp}}$  is the full Hamiltonian of the isolated impurity atom (or ion), and  $H_{kd}$  is a one-body operator which allows for the mixing of the conduction electron state  $\mathbf{k}$  with an electron in one of the virtual  $d$  levels. Normally,  $H_{kd}$  is taken to be of the form

$$\sum_{\mathbf{k}\sigma} V_{kd} c_{k\sigma}^+ c_{d\sigma} + V_{kd}^* c_{d\sigma}^+ c_{k\sigma}, \quad (2)$$

where  $V$  describes the strength of the mixing,  $c_{k\sigma}^+$  creates a conduction electron of momentum  $\mathbf{k}$ , spin index  $\sigma$ ,  $c_{d\sigma}$  destroys a  $d$  state electron of spin index  $\sigma$ , and the other quantities are their conjugates. The width of the virtual  $d$  levels  $\Gamma$  is related to  $V_{kd}$  and  $\rho$ , the density of states per spin state at the Fermi surface on the host metal, by<sup>24,28</sup>

$$\Gamma = \pi \rho |V_{kd}|_s v^2, \quad (3)$$

where the average is over  $\mathbf{k}$  states at the Fermi surface.

A large part of the recent theoretical activity in the field of localized moments has been based on a sequence of papers by Kondo,<sup>33,36,37</sup> who starts with the assumption that a moment exists, and characterizes the impurity by simply assigning it a spin  $\mathbf{S}$ , which interacts with the conduction electrons through a contact interaction represented by a term in the Hamiltonian

$$H_{\text{ex}} = -J\Omega\mathbf{S} \cdot \mathbf{s}(0) \quad J < 0, \quad (4)$$

where  $J$  is the strength of the exchange interaction,<sup>38</sup>  $\Omega$  is an atomic volume, and  $\mathbf{s}(0)$  is the average con-

duction electron spin density at the impurity. For a matrix crystal containing  $N$  atoms, this may be written in terms of conduction electron creation and annihilation operators  $c_{k\sigma}^+$  and  $c_{k\sigma}$  as

$$H_{\text{ex}} = -(J/2N) \sum_{\mathbf{k}, \mathbf{k}'} [(c_{k\downarrow}^+ c_{k'\downarrow} - c_{k\downarrow} c_{k'\downarrow}) S_- + c_{k\uparrow}^+ c_{k'\uparrow} S_+ + c_{k\downarrow}^+ c_{k'\downarrow} S_- + c_{k\uparrow} c_{k'\uparrow} S_+], \quad (5)$$

where  $\mathbf{k}$  and  $\mathbf{k}'$  are the initial and final momenta of the interacting electrons, and  $S_{\pm}$  are raising and lowering operators for the components of  $\mathbf{S}$ .

Attempting to evaluate the contribution of this exchange coupling to the electrical resistivity of alloys containing localized moments, Kondo discovered that the exchange scattering cross section diverges at low temperatures, causing the resistivity to increase logarithmically as the temperature approaches absolute zero. When more sophisticated techniques based on many-body perturbation theory,<sup>18</sup> double time Green's functions,<sup>5</sup> or dispersion theory<sup>15,16</sup> were applied to Kondo's Hamiltonian, it was found that below a certain temperature  $T_K \approx T_F \exp(-1/|J|\rho_1)$ , now called the Kondo or Suhl-Abrikosov temperature, a new electron state should exist. Here  $kT_F = E_F$ , and  $\rho_1$  is the density of states of one spin index *per atom* in the host metal, evaluated at the Fermi surface. Below this temperature, the high-temperature state consisting of conduction band plus localized moment, modified by the weak perturbational exchange coupling between them, collapses to a "quasi-bound state" whose ground state energy at  $T=0^\circ\text{K}$  is approximately  $kT_K$  below that of the same system without the coupling.

The transition to the quasi-bound state is broadened in temperature by thermal fluctuations associated with its small number of degrees of freedom. Since  $kT_K$  goes to zero more rapidly than any power of  $J$  as  $J$  approaches zero, these results explained the difficulties with the perturbational approach. Roughly speaking, the quasi-bound state in this picture consists of the bare high-temperature localized spin clothed in a cloud of conduction electron spin polarization tending to cancel its magnetic moment.

Recently, the dispersion theory calculation has been extended into the region surrounding  $T_K$ ,<sup>18</sup> where all of the earlier work had experienced computational difficulties. These authors also emphasize the important role of the influence of ordinary potential scattering from the impurity on the properties of the quasi-bound state, including the value of  $T_K$ . Silverstein and Duke<sup>39</sup> have demonstrated that below the Kondo temperature, existing theories are valid to at most logarithmic accuracy in the conduction electron energies; to that accuracy, the results of Suhl and Abrikosov are equivalent. These two models, in turn, have been shown to be closely related to that of Nagaoka.<sup>19</sup> (See also a letter

<sup>33</sup> J. Kondo, Progr. Theoret. Phys. (Kyoto) **28**, 846 (1962).  
<sup>34</sup> B. Muhschlegel and J. R. Schrieffer (unpublished work, see Ref. 30).

<sup>35</sup> K. Yosida, A. Okiji, and S. Chikazumi, Progr. Theoret. Phys. (Kyoto) **33**, 559 (1965).

<sup>36</sup> J. Kondo, Progr. Theoret. Phys. (Kyoto) **32**, 37 (1964).

<sup>37</sup> J. Kondo, Progr. Theoret. Phys. (Kyoto) **34**, 204 (1965).

<sup>38</sup> Kondo uses a coupling constant  $J_K = J/2$ .

<sup>39</sup> S. D. Silverstein and C. B. Duke, Phys. Rev. Letters **18**, 695 (1967).

by Suhl.<sup>40</sup>) It has also been shown that the quasi-bound state can be broken up by applying a magnetic field greater than  $H_c$ , where  $\mu_B H_c \approx kT_K$ ,  $\mu_B$  = one Bohr magneton.<sup>1,41,42</sup>

Using the exchange model in a simple variational calculation, it can be demonstrated that a spin  $\frac{1}{2}$  local moment plus a conduction electron form a singlet in their variational ground state.<sup>8</sup> Such a ground state can also be found in a many-body calculation.<sup>13,20,43</sup> Using a model that results in a spin-degenerate zero-temperature ground state, Kondo has shown that the usual susceptibility obtained at  $T=0$  in the singlet calculations,<sup>13,20</sup>  $\chi \approx \mu_B^2/kT_K$ , can also be a property of non-singlet models. Susceptibility results using a Green's function technique show a large reduction in the total moment of the quasi-bound state<sup>6</sup> at low temperatures, as do the experimental data,<sup>1-4</sup> but the question of the existence of a singlet ground state at absolute zero is still open.<sup>19,44</sup>

By performing a canonical transformation on the Anderson Hamiltonian to remove the  $H_{kd}$  term to first order in  $V_{kd}$ , the mixing term can be put into the form of Kondo's exchange Hamiltonian<sup>30</sup> if  $\Gamma/\epsilon_d \ll 1$ . As mentioned earlier, this is likely to be a good approximation in cases in which localized moments occur at all. The relation between the Anderson model and the exchange model is then expressed by the relation:

$$J/N = -2[|V_{kpd}|_av^2 U / (|\epsilon_d| \cdot |\epsilon_d + U|)], < 0 \quad (6)$$

where the normalization of  $J$  is that of Eqs. (4) and (5).

## II. CHARACTERISTIC TEMPERATURES: THE EXPERIMENTS

Formation of a quasi-bound state of the type discussed by Nagaoka, Suhl, Abrikosov, Yosida, and others<sup>5-20</sup> manifests itself in many of the observable properties of alloys containing localized magnetic impurity states. Theories exist which allow the Kondo temperature  $T_K$  appearing as a parameter in various calculations to be related quantitatively to temperatures characteristic of the experimental data but rarely

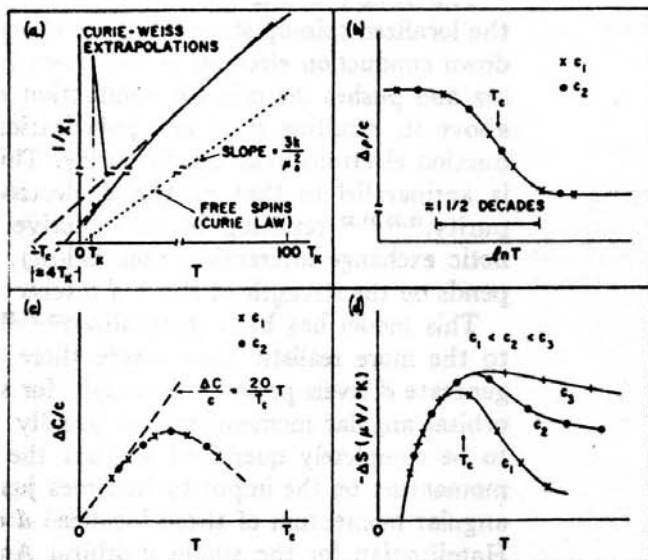


FIG. 1. Typical behavior of the incremental susceptibility, resistivity, specific heat, and thermoelectric power resulting from the addition of various small concentrations  $c_1$ ,  $c_2$ , and  $c_3$  of a magnetic impurity to a nonmagnetic host metal. The features of the inverse susceptibility curve (a) are exaggerated to show small deviations from the Curie-Weiss law, as discussed in the text. It is important to note that  $T_c$  is a characteristic temperature used to facilitate the correlation of several properties of the alloys. Its precise relation to the transition temperature  $T_K$  appearing in various theories depends on the structure of the theory chosen.

experiments available. As will be seen later, the exponential nature of the variation of  $T_c$  from alloy to alloy minimizes the importance of uncertainties of factors of 2,  $\pi$ , etc. in the theories and in the assigned values of  $T_c$ . However, the rules used to obtain values of  $T_c$  are carefully spelled out, so that the results of the present compilation may be readily compared with theoretical relations other than those used here.

A review of the existing experimental work covering the first-row transition elements as impurities in copper and gold reveals some striking systematic relationships. An understanding of the reasons for these orderly variations of  $T_c$  (and hence  $T_K$ ) from alloy to alloy should be useful in explaining the fundamental properties of localized moments in metals. Only for a very few

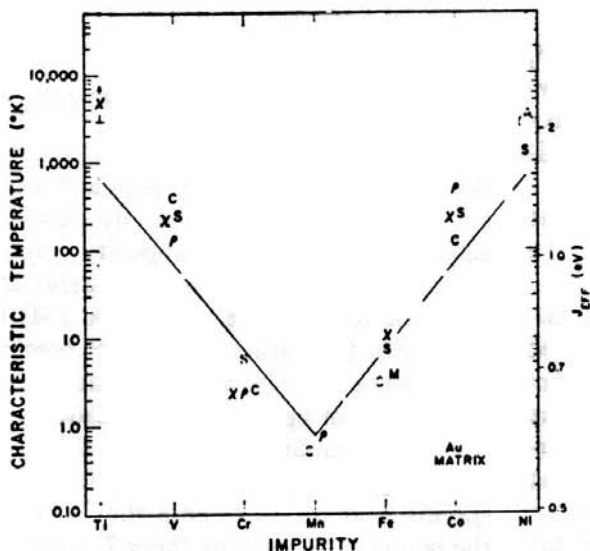


FIG. 2. Characteristic temperatures for first-row transition elements in gold. Values are obtained from data in alloys sufficiently dilute that impurity-impurity interactions are not important, and therefore are properties of the impurity-matrix interaction itself. Symbols used to represent each type of measurement are: susceptibility,  $\chi$ ; resistivity,  $\rho$ ; specific heat, C; thermoelectric power, S; Mössbauer, M; and infrared absorption, A. Light broken symbols indicate a result uncertain to more than a factor of 2. The temperatures  $x$  and M are probably high estimates of  $T_K$  (see text).  $J_{eff}$  is from Eq. (10), using  $\rho_1 = 0.15 \text{ eV}^{-1} \text{ atom}^{-1}$  in both gold and copper. Straight lines represent Eq. (14).

enough of the impurity was present to permit a meaningful number to be obtained. Every attempt was made to establish concentration independence of the contribution per impurity of each property of each alloy (see appendix). In this way impurity-impurity interaction effects appearing at low temperatures were largely avoided.

### A. Susceptibility

Perturbation calculations of the temperature-dependent part of the susceptibility contribution of each impurity approach the limit  $\chi_i = \mu_e^2 / 3kT$  at temperatures far above  $T_K$ .<sup>45,46</sup> Here  $\mu_e$  is the effective number of Bohr magnetons,  $\mu_e^2 = g^2 [S(S+1)] \mu_B^2$ , of an impurity of spin  $S$ , Landé g factor  $g$ . Below  $T_K$ , no detailed calculations of  $\chi_i$  have been made except for its value at  $T=0$ ,<sup>5,19,20,43</sup> which, according to several authors<sup>20,43</sup> can be taken as approximately  $\mu_e^2 / 3kT_K$ . A Curie-Weiss law of the form

$$\chi_i = (\mu_e^2 / 3k)(T + T_K)^{-1} \quad (7)$$

is a convenient choice for an interpolation formula between these two limits, and Kondo<sup>43</sup> has recently given theoretical reasons for expecting the susceptibility to be of this form. Values used in the present analysis for the temperatures characteristic of the susceptibility were obtained by fitting a law of the above form (with  $T_c$  substituted for  $T_K$ ) to the data, and are

<sup>45</sup> D. J. Scalapino, Phys. Rev. Letters 16, 937 (1966).

<sup>46</sup> D. R. Hamann, Phys. Rev. Letters 17, 145 (1966); L. Dvorin, *ibid.* 16, 1042 (1966).

represented in Figs. 2-4 by the symbol  $x$ .<sup>47</sup> Usually,  $T_c$  was obtained by plotting the reciprocal of the susceptibility per impurity atom versus  $T$ , and extrapolating to  $1/\chi_i = 0$ ,<sup>48</sup> where  $T = -T_c$  [Fig. 1(a)].

### B. Resistivity

Theory<sup>5,15,19</sup> and experiment have shown that the thermal breakup of the quasi-bound state with increasing temperature will generally be accompanied by a drop in the impurity contribution to resistance ( $\Delta\rho = \rho_{\text{alloy}} - \rho_{\text{pure}}$ ) as shown in Fig. 1(b). (The resistance of the host,  $\rho_{\text{pure}}$ , increases with  $T$ , primarily because of electron-lattice scattering.) Ideally, the characteristic temperature could be taken at the mid-

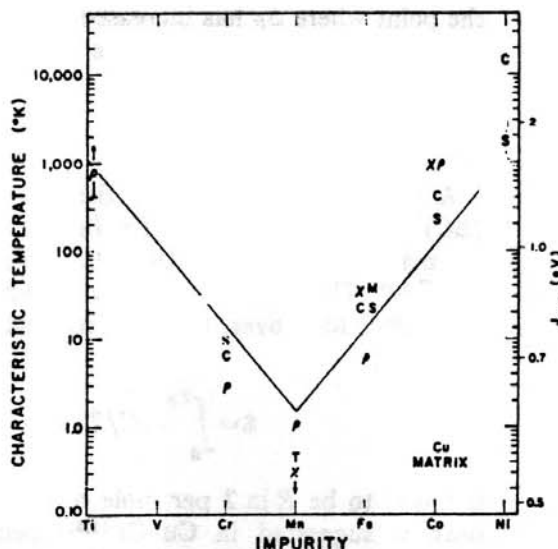


FIG. 3. Characteristic temperatures for first-row transition elements in copper. See Fig. 2 caption.

<sup>47</sup>  $\chi_i = (\chi_{\text{alloy}} - \chi_{\text{pure}})$  per gram divided by the number of impurity atoms per gram. In these matrices  $\chi_{\text{pure}}$  is an approximately temperature independent negative quantity.

<sup>48</sup> It should be pointed out that one can do better than this in individual cases by using the complete expression for  $\chi$  from perturbation theory (Ref. 45) which can be put in the form:

$$1/\chi_i = [\mu_e^2 / 3kT_K]^{-1} \tau [\ln \tau / (\ln \tau - 1)], \quad [\tau = T/T_K].$$

This expression, shown schematically in Fig. 1(a), is a very slowly varying function of  $\tau$  above  $\tau = 8$ , being slightly concave downward above  $\tau = 15$ . It has a divergence at  $\tau = e$ , and is probably unphysical below about  $\tau = 10$ . The true  $1/\chi_i$  function is expected to drop at  $T=0$  to at least  $[\mu_e^2 / 3kT_K]^{-1}$  and possibly to 0. Making the reasonable assumption that the curve remains concave downward throughout its range, and using the known behavior of the CuFe susceptibility (Refs. 4 and 49) as a model in the region near  $T_K$  (or  $\tau = 1$ ), it is possible to draw the solid curve shown. For the range of temperatures covered in a typical experiment carried out above about  $3T_K$ , this function approximates a Curie-Weiss law quite well. In general, this law will have the form:

$$\chi_i = [(a\mu_e)^2 / 3k] / (T + bT_K),$$

where for the range  $4T_K < T < 100T_K$ , for example,  $a = 0.90$ ,  $b = 4$ . Thus, for low values of  $T_K$ ,  $T_c$  determined from the Curie-Weiss law probably overestimates  $T_K$  by a factor of four, while the values obtained for  $\mu_e$  underestimate the true effective moment by about 10%. These model-dependent corrections have not been applied to any of the numbers presented in this paper but should be kept in mind.

<sup>49</sup> C. M. Hurd, J. Phys. Chem. Solids 28, 1345 (1967); Phys. Rev. Letters 18, 1127 (1967).

point of the ramp. However, except for Cu-Fe<sup>4</sup>, Cu-Cr<sup>49a</sup> and possibly Zn-Mn<sup>50</sup> only the high- or low-temperature knee of the expected curve is seen. By assigning a height to this step we can estimate the midpoint when only a portion of the curve is known.

In the absence of a comprehensive theory the height of the step has been taken to be independent of the impurity material.

The change at the step is observed to be 0.14 nΩ-cm/at ppm (1.4 μΩ-cm/at.%) in Cu, and calculated to be 0.16 nΩ-cm/at ppm in Au and 0.07 nΩ-cm/at ppm in Mg, Cd, and Zn, using the prediction<sup>5,19</sup> that the step height scales as  $E_F^{-1/2}$ . The characteristic temperature ( $\varrho$  in Figs. 2-4) is *defined* as the temperature at the point where  $\Delta\rho$  has increased or decreased from its temperature independent value by  $\frac{1}{2}$  the size of the above change.

### C. Specific Heat

A peak is anticipated in the excess specific heat ( $\Delta C$ ) between  $T=0$  and  $T=T_K$  associated with the thermal destruction of the quasi-bound state [Fig. 1(c)].<sup>5,19</sup> This peak is clearly observed at 6°K in Cu-Fe.<sup>51,52</sup> Moreover, the entropy associated with the state,

$$S = \int_0^{T_K} \Delta C/T dT,$$

is found to be  $R \ln 2$  per mole of impurity. A similar peak is suggested in Cu-Cr<sup>52,53</sup> specific heat data, where  $S$  is  $R \ln 2.5$  per mole of impurity. ( $R$  is the gas constant per mole.)

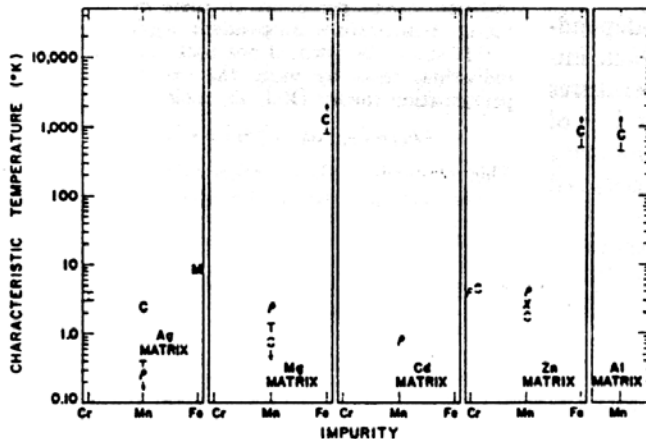


FIG. 4. Characteristic temperatures for first-row transition elements in silver, magnesium, cadmium, zinc, and aluminum. See Fig. 2 caption.

<sup>48a</sup> M. D. Daybell and W. A. Steyert, Phys. Rev. Letters 20, 195 (1968).

<sup>49</sup> F. T. Hedgcock and C. Rizzuto, Phys. Rev. 163, 517 (1967).

<sup>50</sup> J. P. Franck, F. D. Manchester, and D. L. Martin, Proc. Roy. Soc. (London) A263, 494 (1961).

<sup>51</sup> F. J. du Chatenier and J. de Nobel, Physica 32, 1097 (1966).

<sup>52</sup> F. J. du Chatenier and A. R. Miedema, Physica 32, 403 (1966).

Nagaoka predicts that

$$\Delta C/cT \mid_{T \rightarrow 0} \rightarrow 2.39R/T_K, \quad (8)$$

where  $c$  is the impurity concentration. A similar expression has been obtained by Kondo,<sup>43</sup> with a constant of 6.6 instead of 2.39. Thus, by observing  $\Delta C/cT$  at sufficiently low  $c$  to avoid impurity-impurity interaction effects and for  $T \ll T_K$ , we can arrive at another characteristic temperature (C in Figs. 2-4) by using  $T_c$  for  $T_K$  in Eq. (8). Other theories<sup>19,44</sup> predict a different  $T$  dependence of  $\Delta C/c$  as  $T \rightarrow 0$ , and it has been pointed out<sup>53a</sup> that an approximation made by Nagaoka casts some doubt on his calculation of this quantity. Because the energy of a system is such a fundamental quantity, specific heat measurements should reveal much about the bound state, making these  $T_c$ 's of basic importance. Unfortunately, arriving at numbers for C based on its definition involves more interpretation and uncertainty than any of the other characteristic temperatures. This is because the measurements must be made at low temperatures (generally less than 20°K) and high concentration (generally greater than 0.1%) so that  $\Delta C$  is not completely masked by the host specific heat. Hence, it is hard to be completely free of impurity-impurity interactions for spins with large magnetic moments at low temperatures (i.e., systems with  $T_c < 100^{\circ}\text{K}$ ).

For systems with higher  $T_c$ 's, however, interactions are not so important and the  $\Delta C \propto cT$  behavior of the low-temperature limit is seen. This appears as an increase in the electronic specific heat parameter  $\gamma$  ( $C = \gamma T + \alpha T^3$ ). In the past this change has generally been interpreted from the band theory point of view as due to a change,  $\Delta\rho_1$ , in the density of electronic states ( $\rho_1$ ) at the Fermi surface. It has been observed, however, that the  $\Delta\rho_1$  obtained from what has been considered to be a change in the Pauli susceptibility upon alloying differs by a factor of about 4 from the  $\Delta\rho_1$  arrived at from the change in  $\gamma$ , both in Cu-Ni<sup>54</sup> and Au-V.<sup>55</sup> Considering the observed changes in  $\chi$  and  $\gamma$  as due to the high temperature bound state phenomenon is one way of resolving this discrepancy.<sup>56</sup>

### D. Thermoelectric Power

Suhl and Wong<sup>18</sup> predict that there will be a concentration independent peak in the thermoelectric power of a dilute magnetic alloy near  $T_K$ . In practice, enough of the magnetic impurity must be present for its exchange scattering contribution to dominate the thermopower, in which case a dramatic peak is observed whose

<sup>53a</sup> P. E. Bloomfield (preprint); D. S. Falk and M. Fowler, Phys. Rev. 158, 567 (1967).

<sup>54</sup> E. W. Pugh, B. R. Coles, A. Arrott, and J. E. Goldman, Phys. Rev. 105, 814 (1957).

<sup>55</sup> F. J. du Chatenier, J. de Nobel, and B. M. Boerstoel, Physica 32, 561 (1966).

<sup>56</sup> Equation (7) is used for  $\Delta\chi$  with the  $T_c$  (= 16,000°K in Cu-Ni and 400°K in Au-V) determined from the  $\Delta C$  data. The magnitude of  $\Delta\chi$  can be fit by a value of  $3.2 \mu_B$  for  $\mu$  in both systems. See also a complementary scheme by A. P. Klein and A. J. Heeger, Phys. Rev. 144, 458 (1966).

magnitude and position are more or less independent of concentration and whose shape is approximately gaussian in  $\log T$ , as predicted. At high concentrations the shape of the peak changes, as shown schematically in Fig. 1(d), so that some judgment enters into choosing the proper range of concentrations from which to obtain a characteristic temperature, at least if high accuracy is desired.<sup>57</sup> The temperature at which the peak (denoted by S in Figs. 2 and 3) occurs in a suitably chosen concentration range of the alloy is defined as the  $T_c$  for the thermopower. The effect of the small and positive increase of the thermopower of the host metal with  $T$  is unimportant and has been ignored.

### E. Other Measurements

Using the Mössbauer effect, the magnetic character of dilute Fe impurities in various host matrices can be studied. The effective internal magnetic field,  $H_i$ , at the Fe nucleus due to polarization of its electronic environment is measured in an external magnetic field. This polarization deviates appreciably from its high temperature  $1/T$  behavior at a characteristic temperature ( $M$  in Figs. 2-4) given by the phenomenological parameter  $[(J+1)/J]_s$  used in the Mössbauer work.<sup>58</sup> However,  $H_i$  does not differ significantly from its high temperature  $1/T$  behavior until  $T$  is down to about a third of this characteristic temperature so that  $M$  is probably a high estimate of  $T_K$ .

A peak appears in the infrared absorption by Au-Ni films<sup>59</sup> at photon energies which vary from 0.5 to 0.8 eV as  $c$  is varied from 3.9% to 10.2%. Its magnitude is proportional to  $c$ . Our linear extrapolation of that data indicates that the position of the peak as  $c \rightarrow 0$  would be 0.32 eV corresponding to a 3700°K binding energy for the quasi-bound state in Au-Ni (A in Fig. 2).

The tunneling of electrons from a superconductor to a dilute alloy can be used to observe the expected anomaly<sup>60</sup> in the density of states at the Fermi surface in these alloys.<sup>60,61</sup> The quasi-bound states also affect other properties of dilute alloys such as thermal conductivity, expansion coefficient, ESR, NMR, DeHaas-Van Alphen and Hall effects, superconducting transition temperatures, and magnetoresistivity.<sup>21</sup>

<sup>57</sup> Ideally a sequence of Nordheim-Gorter diagrams [see D. K. C. MacDonald, *Thermoelectricity* (John Wiley & Sons, Inc., New York, 1962), p. 109] for various concentrations of impurity at several temperatures would be used to extrapolate the thermoelectric power at each temperature; the peak in the graph of the values obtained vs. the temperature would then be taken as  $T_c$ .

<sup>58</sup> T. A. Kitchens, W. A. Steyert, and R. D. Taylor, Phys. Rev. 138, A467 (1965).

<sup>59</sup> F. Abeles, in *Metallic Solid Solutions*, J. Friedel and A. Guinier, Eds. (W. A. Benjamin, Inc., New York, 1963), Chap. 17, p. 1.

<sup>60</sup> F. T. Hedcock and C. Rizzuto, Phys. Letters 24A, 17 (1967).

<sup>61</sup> J. A. Appelbaum, Phys. Rev. Letters 17, 91 (1966); Phys. Rev. 154, 633 (1967); P. W. Anderson, Phys. Rev. Letters 17, 95 (1966).

### III. A SIMPLE MODEL

Almost none of the theoretical effort dealing with the localized moment problem has been concerned with the problem of predicting the magnitude of the Kondo coupling constant  $J$ , or its behavior as a function of the position of a given impurity in the periodic table (see, however, Ref. 62). As Suhl<sup>16,18</sup> has pointed out, even knowing  $J$  would not imply that  $T_K$  could be calculated directly from the expression

$$T_K \approx T_F \exp(-1/|J| \rho_1) \quad (9)$$

since effects caused by potential scattering off of the same impurity responsible for the exchange scattering will modify the above formula. Nevertheless, it is useful to use the above expression to *define* an effective exchange constant  $J_{\text{eff}}$  by

$$T_K = T_F \exp(-1/|J_{\text{eff}}| \rho_1). \quad (10)$$

For an estimate of  $J_{\text{eff}}$ , we ignore the possibility that it may differ significantly from  $J$ , and turn to a recent calculation by Schrieffer<sup>12</sup> in which, by applying the canonical transformation technique<sup>30</sup> to a generalization of the Anderson model that accommodates all ten  $d$  electron levels, an expression is obtained which can be used to find the dependence of  $J$  on the total spin value of the "bare" localized moment. In that paper, it is pointed out that  $J$  should arise primarily from a resonant interaction between the  $d$ -wave part of the conduction electron wave functions and the localized  $d$  states on the impurity, rather than from the  $s$ -wave- $d$ -state interaction assumed in most other calculations.<sup>63</sup> The  $n$   $3d$  electrons of the impurity are assumed to occupy the available  $d$  level according to Hund's rule, so that the localized spin  $S = n/2$  for  $n \leq 5$ , and is  $(10-n)/2$  for  $n \geq 5$ . The  $n_u$  ( $= 2S$ ) unpaired electrons go into the  $d$  orbitals of angular momentum magnetic quantum number  $m_1 = L$ ,  $m_2 = L-1$ ,  $m_3 = L-2 \dots m_u$ ; the ground state of the unperturbed impurity is an eigenstate of the total orbital angular momentum operator,  $L^2$ . Spin-orbit and orbital exchange interactions with the conduction band are neglected. Schrieffer points out that with these assumptions, only conduction electrons having the same  $d$ -wave magnetic quantum number,  $m$ , as one of the singly occupied  $d$  orbitals on the impurity can undergo spin-spin exchange scattering of the Kondo type. Under these conditions,

$$J_m/N = -[|V|^2/|\epsilon_m|][U/|\epsilon_m + U|][2S]^{-1}, \quad (11)$$

where  $U$  and  $V$  are analogs of the Coulomb and  $s-d$  mixing integrals of the single orbital Anderson model, although here  $V$  is expressed in terms of conduction band states which are eigenfunctions of the orbital

<sup>62</sup> R. E. Watson, S. Koide, M. Peter, and A. J. Freeman, Phys. Rev. 139, A167 (1965).

<sup>63</sup> See Refs. 12 and 62 for a further discussion of this point.

angular momentum, rather than Bloch functions. The constant  $J_m$  is the analog of  $J$  in Eq. (5) and can be defined by replacing the conduction electron operators in that equation by those for band states of angular momentum  $l=2$ ,  $l_s=m$ , wave number  $k$ , spin  $\pm\frac{1}{2}$ . The Kondo temperature is still given by Eq. (9), with  $J$  replaced by  $J_m$ . The energy required to remove an electron from a singly occupied  $d$  orbital and place it at the Fermi energy,  $-|\epsilon_m|$ , is assumed to be independent of  $m$ . Using the fact that  $\epsilon_m \approx -U/2$  if a localized moment is to occur at all in the Anderson model (unless the virtual level is quite narrow),

$$J_m \rho / N = -2\rho |V|^2 / n_u |\epsilon_m| \quad (12)$$

or, by comparison with Eqs. (3) and (6),

$$|J_m| \rho_1 = 4\Gamma / n_u \pi |\epsilon_m|. \quad (13)$$

Using these results of Schrieffer's analysis, we make the simplest choice of  $\Gamma/|\epsilon_m|$  consistent with the features of the experimental results, and set it equal to a constant, independent of the position of the impurity atom in the first row transition series. Inserting Eq. (13) in Eq. (7) gives:

$$\ln T_K = -\pi(|\epsilon_m|/4\Gamma)n_u + \ln T_F. \quad (14)$$

If  $n_u$  is alloyed to change in integer steps starting at 2 in titanium, increasing to 5 in manganese, and then decreasing to 2 again in nickel, the curves shown in Figs. 2 and 3 are obtained when  $\Gamma/|\epsilon_m|$  is taken to be 0.306 in copper and 0.309 in gold.

Several features of this admittedly crude calculation should be pointed out. First, it provides a very good qualitative description of the impurity dependence of  $T_K$ . In the two systems examined,  $\Gamma/|\epsilon_m|$  is nearly constant; allowing it to vary by  $\pm 15\%$  from impurity to impurity would bring the predictions of the model into quantitative agreement with the experiments. The half-width  $\Gamma$  of the virtual level is only about 30% of its distance below the Fermi level, so that the requirements for the exchange model to be equivalent to the Anderson model are reasonably well satisfied. Since  $\ln T_F$  varies only slightly on the scale of Figs. 2-4 as the Fermi energy changes from 5.5 (for gold) to 14 eV (for aluminum), the principal effect of Friedel's assumption<sup>23,24</sup> that  $\Gamma/|\epsilon_m|$  increases with  $E_F$  is to push the center of the V-shaped curve upward at higher Fermi energies while its ends remain fixed. This is consistent with Schrieffer's explanation of the behavior of the room-temperature residual resistivity of dilute alloys of the first-row transition elements in aluminum, in which it is assumed that the Kondo temperature of each of these alloys lies above the temperature of the measurements.<sup>12</sup> On this model, the aluminum alloys form a degenerate case of the class of materials discussed above. In the aluminum system, moreover, the maximum value of  $n_u$  occurs near chromium rather than

near manganese, where it apparently occurs in copper and gold alloys. This may be explained by valency effects arising from the smaller electronegativity of aluminum, which would tend to increase the number of  $d$  electrons on the transition impurities.

Such a trend in the position of the maximum value of  $n_u$  with electronegativity also seems to be present in the fragmentary data on the other systems shown in Fig. 4, and possibly even in copper, where it appears that the "vee" curve in Fig. 2 might better represent the results if  $n_u$  were allowed to reach its maximum somewhere between chromium and manganese.

#### IV. DISCUSSION

By examining the experimental literature covering a few relatively well-studied alloy systems in the light of recent theoretical ideas, it has been possible to assemble a great deal of evidence for the conjecture that the Kondo effect, and in particular the quasi-bound state, forms the link between magnetic and nonmagnetic impurities in metals. The beginnings of a quantitative understanding of the mechanism involved, contained in a crude model involving many simplifying assumptions, make it possible to predict, in systems for which sufficient information exists, the temperature  $T_K$  near which the transition between these two types of states will occur. Experiment and theory together make it clear that the quasi-bound state phenomenon is widespread, and is definitely not restricted to low temperatures.

These developments make it necessary to revise the picture of transition metals as impurities in metals. A few alloys, like Cu-Co and Au-Co, which have been considered to be nonmagnetic,<sup>24</sup> must be considered from this more general point of view. Information presented here should be useful in reaching a better theoretical understanding of the dependence of properties of dilute alloys such as residual resistivity on the position of the impurity in the periodic table. Experiments<sup>25</sup> in ternary alloys where local moments on a transition-metal impurity appear and disappear as the electron concentration of the binary matrix is varied may be explained by the rapid variation of  $T_K$  with  $J_{eff}$ .

The Kondo effect is apparently not sensitive to the state of order of the matrix, as evidenced by its existence at temperatures where lattice vibrations dominate the electrical resistance and specific heat, and by the fact that resistivity minima have been seen in copper-gold alloys containing traces of iron, and these minima remain even when the alloy is transferred from the ordered to the disordered phase.<sup>26</sup> It would be surprising

<sup>23</sup> G. J. van den Berg, Paper A68, given at the 10th International Conference on Low Temperature Physics, Moscow (1966).

<sup>24</sup> A. M. Clogston, B. T. Matthias, M. Peter, H. J. Williams, E. Corenzwit, and R. C. Sherwood, Phys. Rev. 125, 541 (1962).

<sup>25</sup> M. Hirabayashi and Y. Muto, Acta Met. 9, 497 (1961).

TABLE II. Measured effective magnetic moments  $\mu_e$  of transition metal impurities in various matrices, expressed in Bohr magnetons.  $\mu_e = g[j(j+1)]^{1/2}$ , where  $j$  is the total impurity angular momentum and  $g$  is the Lande  $g$  factor.

Matrix	V	Cr	Mn	Fe	Co
Au	3.1 <sup>a</sup>	4.0 <sup>b</sup>	5.8 <sup>b</sup>	3.7 <sup>c</sup>	4.5 <sup>d</sup>
Ag			5.6 <sup>e</sup>		
Cu		3.9 <sup>f</sup>	4.9 <sup>g</sup>	3.7 <sup>g</sup>	3-5 <sup>d</sup>
Cd			3.8 <sup>h</sup>		
Zn			3.9 <sup>i</sup>		
Mg			5.2 <sup>j</sup>		

<sup>a</sup> Reference 3.

<sup>b</sup> Reference 69.

<sup>c</sup> Reference 49.

<sup>d</sup> Reference 70.

<sup>e</sup> Reference 71.

<sup>f</sup> Reference 72.

<sup>g</sup> Reference 21.

<sup>h</sup> Reference 50.

<sup>i</sup> Reference 74.

<sup>j</sup> Reference 75.

if dilute alloys of liquid metals did not exhibit a Kondo effect as well.

There are some oversimplifications in the picture presented in Sec. III. In Au-Fe, for example, the residual resistivity begins to drop again a few hundred degrees below its melting point,<sup>67</sup> while in at least one typical nontransition metal alloy, Au-Al, it is rising in this region.<sup>68</sup> Other data (particularly the susceptibility) are not consistent with this being some sort of "second Kondo effect," and it may even be an oxidation or metallurgical problem. More data are needed.

Another problem is that the simple choice made for  $n_u$ , the number of unpaired spins, in Sec. III is only in qualitative agreement with the spin values determined from susceptibility results<sup>3,21,49,50,69-75</sup> (Table II).

Some of these discrepancies undoubtedly arise from the fact that a large percentage of the measurements available are not ideally adapted to the type of analysis needed to discuss the Kondo effect. Much experimental work needs to be done on each of the alloys in which a localized magnetic state is believed to exist, with appropriate care taken to establish absence of problems caused by interactions, precipitation of solute on cooling, oxidation of the impurity caused by overlong

<sup>a</sup> C. A. Domenicali and E. L. Christenson, J. Appl. Phys. 32, 2450 (1961).

<sup>b</sup> M. D. Daybell, D. L. Kohlstedt, and W. A. Steyert, Solid State Commun. 5, 871 (1967). The resistivity behavior can apparently be explained by phonon-electron interactions. U. Herbst and D. Wagner (preprint); and Phys. Letters 25A, 251 (1967).

<sup>c</sup> O. S. Lutes and J. L. Schmit, Phys. Rev. 134, A676 (1964).

<sup>d</sup> E. Hildebrand, Ann. Physik (5) 30, 593 (1937); E. Daniel, J. Phys. Chem. Solids 23, 975 (1962).

<sup>e</sup> G. Gustafsson, Ann. Physik (5) 25, 545 (1936).

<sup>f</sup> L. Creveling (unpublished work).

<sup>g</sup> A. R. Kaufmann and C. Starr, Phys. Rev. 63, 445 (1943).

<sup>h</sup> E. W. Collings, F. T. Hedgcock, and Y. Muto, Phys. Rev. 134, A1521 (1964).

<sup>i</sup> E. W. Collings and F. T. Hedgcock, Phys. Rev. 126, 1654 (1962).

annealing<sup>76-78</sup> (even in a good vacuum), and other spurious effects. Studies using a binary alloy as the matrix would be of interest, as would data on liquid metals. Other transition metals and the rare earth series as solutes have not yet been extensively studied. The combination of the Kondo effect with superconductivity, using suitable solvent metals, is beginning to be investigated, but certainly much more of interest remains to be learned.<sup>79,80</sup>

Another interesting question involves alloys such as Fe in Rh and Ir where the impurity contribution to resistance increases with increasing temperature.<sup>81</sup> This has been discussed in terms of a positive  $J$ . However, these alloys show a susceptibility like that of Fig. 1(a), indicating a very substantial *decrease* in the magnetic moment at low temperatures.<sup>82</sup> Low concentrations of Fe in Rh show a specific heat anomaly at low temperatures,<sup>81</sup> and there are Mössbauer anomalies similar to that in Cu-Fe in the Rh and Ir systems.<sup>58,83</sup> Thus, except for resistivity, these results look like the negative  $J$  systems. Apparently, quasi-bound state formation in these transition metal hosts decreases the scattering of their  $d$ -band conduction electrons, but these systems are only beginning to be understood.<sup>82a</sup>

The analysis of the experiments has reached the point where more detailed theoretical expressions for the various measurable quantities for all temperatures are needed, with careful attention to numerical details and, where possible, estimates of the magnitude of important theoretical parameters. More theoretical results are needed for impurity spin greater than  $\frac{1}{2}$ .

#### ACKNOWLEDGMENTS

We would like to acknowledge communication of their results prior to publication by the following: K. Kume; J. Kondo; H. Suhl and D. Wong; R. B. Frankel, N. A. Blum, B. B. Schwartz, and D. J. Kim; F. Hedgcock and C. Rizzuto; C. Hurd; A. Heeger and M. Jensen; H. Ishii and K. Yosida; and D. Hamann. The authors would also like to express their gratitude for helpful discussions with Dr. L. Gruenberg.

<sup>76</sup> U. Gonser, R. W. Grant, A. H. Muir, Jr., and H. Wiedersich, Acta Met. 14, 259 (1966).

<sup>77</sup> D. H. Howling, Phys. Rev. 155, 642 (1967).

<sup>78</sup> F. J. Norton and A. U. Seybolt, Trans. AIME 230, 595 (1964).

<sup>79</sup> A. Griffin, Phys. Rev. Letters 15, 703 (1965); K. Maki, Phys. Rev. 153, 428 (1965).

<sup>80</sup> G. Boato, G. Gallinaro, and C. Rizzuto, Phys. Rev. 148, 353 (1966). This paper contains references to earlier work.

<sup>81</sup> B. R. Coles, Phys. Letters 8, 243 (1964); and (private communication). B. R. Coles, J. H. Waszink, and J. Loram, in *Proceedings of the International Conference on Magnetism: 1964* (Institute of Physics, London, 1964), p. 165.

<sup>82</sup> G. S. Knapp, J. Appl. Phys. 38, 1267 (1967), and references therein.

<sup>83</sup> R. D. Taylor and W. A. Steyert, J. Appl. Phys. 37, 1336 (1966).

<sup>83a</sup> G. S. Knapp, Phys. Letters 25A, 114 (1967).

## APPENDIX

**Susceptibility data.** Concentration-independent values for  $T_c$  could be accurately determined for Au-Fe,<sup>49,69,71</sup> Au-Co,<sup>70</sup> Au-Cr,<sup>69</sup> Cu-Fe,<sup>49</sup> Cu-Co,<sup>70</sup> and Zn-Mn,<sup>74</sup> where a number of low concentration alloys gave the same  $T_c$ . The impurity susceptibility of Au-Ti<sup>84</sup> and Au-Ni<sup>85</sup> above 100°K showed little temperature variation, thus the extrapolation [Fig. 1(a)] to  $1/\Delta\chi_i=0$  is inaccurate, as indicated in Fig. 2. In Au-V<sup>3</sup> only a 1% alloy has been studied, but interactions should not be important at this concentration in the temperature range of interest, i.e., 200° to 900°K. For Cu-Mn,<sup>21</sup> alloys of 0.029% Mn show  $T_c=0 \pm 0.5$ °K, while a factor of 6 or 7 increase in  $c$  changes this value only slightly. Thus  $T_c$  at the zero concentration limit is unlikely to be greater than 0.5°K, as indicated in Fig. 3.

**Resistivity data.** Clear concentration-independent values for  $T_c$  are readily obtained for Au-Fe,<sup>86-88</sup> Au-Co,<sup>67</sup> Au-Mn,<sup>86</sup> Au-V,<sup>3</sup> Au-Cr,<sup>86</sup> Cu-Fe,<sup>67,89,90</sup> Cu-Mn,<sup>89</sup> Cu-Co,<sup>67</sup> Cu-Cr,<sup>49a</sup> Mg-Mn,<sup>91,92</sup> Cd-Mn,<sup>50</sup> and Zn-Mn.<sup>50</sup>

In Ag-Mn<sup>93</sup> a long extrapolation of the  $\Delta\rho$  vs  $\ln T$  curve is required, hence only an upper limit on  $T_c$  can be estimated. For Zn-Cr,<sup>24</sup>  $T_c$  is estimated by comparing its behavior to results obtained in Zn-Mn in the same experiment.

**Specific heat.** No difficulty is encountered in establishing limiting low  $T$  and  $c$  values of  $\Delta C/T$  in Au-Co,<sup>93</sup> Au-V,<sup>55</sup> Cu-Fe,<sup>51,52</sup> Cu-Co,<sup>52,96</sup> and Cu-Ni.<sup>52</sup> In some cases, however, it was not clear how to extend to  $T=0$  the lowest temperature data for which interaction ef-

fects are absent. To assist in this extrapolation to  $T=0$ ,  $\Delta C/T$  curves of the alloy under consideration were assumed to be similar to the well established Cu-Fe curves. The area under the extrapolated curves was measured to be sure that  $\int \Delta C/c T dT = S$  lay in the range from  $R \ln 2$  to  $R \ln 5$  (0.7R to 1.6R). For Cu-Cr,<sup>52,53</sup> and Ag-Mn,<sup>52,97</sup> this extrapolation is small, but in Au-Cr<sup>55</sup> the extrapolation is much more difficult; nevertheless, the  $T_c$  arrived at is probably correct to within a factor of 2.

The extrapolation in the cases of Au-Fe,<sup>55,98</sup> Au-Mn,<sup>53,55</sup> Ag-Cr,<sup>52</sup> Mg-Mn,<sup>99</sup> Zn-Cr,<sup>52</sup> and Zn-Mn<sup>52</sup> is uncertain to more than a factor of 2 as indicated in Figs. 2, 3, and 4. The lower limit of  $T_c$  for Zn-Fe<sup>52</sup> is based on a measured  $\gamma$  of 0.65 mJ/mole°K<sup>2</sup> for a 0.1% alloy compared to values primarily between 0.60 and 0.65 for the most recent measurements on pure Zn.<sup>100</sup> A 0.045% alloy of Mn in Al has a  $\Delta C/T$  value of less than  $5 \times 10^{-6}$  cal/mole°K<sup>2</sup>,<sup>101</sup> implying  $T_c > 450$ °K.

**Thermoelectric effect.** A thermoelectric power peak is clearly seen in Au-Co,<sup>102</sup> Au-Fe,<sup>86,103,104</sup> Au-V,<sup>68</sup> Cu-Co,<sup>105</sup> and Cu-Fe.<sup>105,106</sup> In Au-Ni<sup>107</sup> measurements have not been made at enough concentrations to establish  $T_c$  to much better than a factor of 2. In the case of Au-Cr<sup>86</sup> the alloys measured may be concentrated enough that ordering effects are occurring. For Cu-Cr we have averaged the different values from Refs. 89 and 105. The thermopower for the Cu-Ni<sup>105</sup> system is still decreasing rapidly at 1000°K toward an apparent negative peak above its melting point.

<sup>49</sup> E. Vogt and D. Gerstenberg, Ann. Physik (7) **4**, 145 (1959).  
<sup>50</sup> E. Vogt and H. Krueger, Ann. Physik (5) **18**, 755 (1933).  
<sup>51</sup> D. K. C. MacDonald, W. B. Pearson, and I. M. Templeton, Proc. Roy. Soc. (London) **A266**, 161 (1962).

<sup>52</sup> N. E. Alekseevskii and I. P. Gaidukov, Zh. Eksperim. i Teor. Fiz. **31**, 947 (1956) [English transl. Soviet Phys.—JETP **4**, 807 (1957)].

<sup>53</sup> J. S. Dugdale and D. K. C. MacDonald, Can. J. Phys. **35**, 271 (1957).

<sup>54</sup> A. Kjekshus and W. B. Pearson, Can. J. Phys. **40**, 98 (1962).  
<sup>55</sup> G. K. White, Can. J. Phys. **33**, 119 (1955).

<sup>56</sup> F. T. Hedcock, W. B. Muir, and R. Wallingford, Can. J. Phys. **38**, 376 (1960).

<sup>57</sup> D. A. Spohr and R. T. Webber, Phys. Rev. **105**, 1427 (1957).  
<sup>58</sup> A. N. Gerritsen and J. O. Linde, Physica **17**, 573 (1951).

<sup>59</sup> Y. Muto, J. Phys. Soc. Japan **15**, 2119 (1960).  
<sup>60</sup> L. T. Crane, Phys. Rev. **125**, 1902 (1962).

<sup>61</sup> L. T. Crane and J. E. Zimmerman, Phys. Rev. **123**, 113 (1961).

<sup>62</sup> F. J. du Chatenier and A. R. Miedema, in *Proceedings of the 9th Conference on Low Temperature Physics*, J. G. Daunt, D. O. Edwards, F. J. Milford, and M. Yaquib, Eds. (Plenum Press, Inc., New York, 1965), p. 1029 (Part B).

<sup>63</sup> B. Dreyfus, J. Soulette, R. Tournier, and L. Weil, Compt. Rend. **259**, 4266 (1964).

<sup>64</sup> D. L. Martin, Can. J. Phys. **39**, 1385 (1961).

<sup>65</sup> Referred to in Ref. 52.

<sup>66</sup> D. L. Martin, Proc. Phys. Soc. (London) **78**, 1489 (1961).

<sup>67</sup> R. L. Powell, L. P. Caywood, Jr., and M. D. Bunch, in *Temperature, Its Measurement and Control in Science and Industry*, C. M. Herzfeld, Ed. (Reinhold Publ. Corp., New York, 1962), Vol. III, Pt. 2, p. 65.

<sup>68</sup> J. J. Schriempf and A. I. Schindler, Cryogenics **6**, 301 (1966).

<sup>69</sup> R. Berman, J. C. F. Brock, and D. J. Huntley, Cryogenics **4**, 233 (1964).

<sup>70</sup> E. L. Christenson, J. Appl. Phys. **34**, 1485 (1963).

<sup>71</sup> G. Borelius, W. H. Keesom, C. H. Johansson, and J. O. Linde, Leiden Commun. **217e**, 34 (1932).

<sup>72</sup> C. A. Domenicali, Phys. Rev. **112**, 1863 (1958).